Cancer Cell
Article

$Kras^{G12D}$-Induced IKK2/β/NF-κB Activation by IL-1α and p62 Feedforward Loops Is Required for Development of Pancreatic Ductal Adenocarcinoma

Jianhua Ling,[1] Ya'an Kang,[2] Ruiying Zhao,[1] Qianghua Xia,[1,4] Dung-Fang Lee,[5] Zhe Chang,[1,4] Jin Li,[6] Bailu Peng,[7] Jason B. Fleming,[2] Huamin Wang,[3,4] Jinsong Liu,[3,4] Ihor R. Lemischka,[5] Mien-Chie Hung,[1,4,8] and Paul J. Chiao[1,4,*]
[1]Department of Molecular and Cellular Oncology
[2]Department of Surgical Oncology
[3]Department of Pathology
The University of Texas M.D. Anderson Cancer Centre, Houston, TX 77030, USA
[4]The University of Texas Graduate School of Biomedical Sciences, Houston, TX 77030, USA
[5]Department of Developmental and Regenerative Biology, and the Black Family Stem Cell Institute, Mount Sinai School of Medicine, New York, NY 10029, USA
[6]Center for Applied Genomics, Children's Hospital of Philadelphia, Philadelphia, PA 19104, USA
[7]Guangdong Entomological Institute, Guangzhou, Guangdong 510260, China
[8]Center for Molecular Medicine and Graduate Institute of Cancer Biology, China Medical University, Taichung 447, Taiwan
*Correspondence: pjchiao@mdanderson.org
DOI 10.1016/j.ccr.2011.12.006

SUMMARY

Constitutive Kras and NF-κB activation is identified as signature alterations in pancreatic ductal adenocarcinoma (PDAC). However, how NF-κB is activated in PDAC is not yet understood. Here, we report that pancreas-targeted *IKK2/β* inactivation inhibited NF-κB activation and PDAC development in $Kras^{G12D}$ and $Kras^{G12D}$;*Ink4a/Arf*$^{F/F}$ mice, demonstrating a mechanistic link between *IKK2/β* and $Kras^{G12D}$ in PDAC inception. Our findings reveal that $Kras^{G12D}$-activated AP-1 induces IL-1α, which, in turn, activates NF-κB and its target genes *IL-1α* and *p62*, to initiate IL-1α/p62 feedforward loops for inducing and sustaining NF-κB activity. Furthermore, IL-1α overexpression correlates with *Kras* mutation, NF-κB activity, and poor survival in PDAC patients. Therefore, our findings demonstrate the mechanism by which IKK2/β/NF-κB is activated by $Kras^{G12D}$ through dual feedforward loops of IL-1α/p62.

INTRODUCTION

The mutational activation of *Kras* is an early event in PDAC development and has been detected in 80%–95% of PDAC, and mutational inactivation of *Ink4a/Arf* tumor suppressor genes can be identified in approximately 50%–75% of PDAC (Hruban et al., 2000). Several experimental animal models were established to determine the functions of mutated *Kras* in induction of pancreatic intraepithelial neoplasia (PanIN) and PDAC (Aguirre et al., 2003; Bardeesy et al., 2006; Hingorani et al., 2003). However, the key signaling pathways that function downstream of *Kras* remained unidentified.

Several previous studies have shown a key role of the NF-κB signaling pathway in Ras-driven cancers using animal models of cancer. For example, knockout of IKK2/β inhibited H-Ras-driven melanoma (Yang et al., 2010), inhibition of NF-κB bypassed restraints on oncogenic Ras-stimulated growth in induction of invasive human epidermal neoplasia (Dajee et al., 2003), and loss of IKK2/β in hepatocyte enhances inflammation, tumor promotion, and progression (He et al., 2010; Maeda et al., 2005). We previously showed that RelA/p50NF-κB is constitutively activated in almost 70% of pancreatic cancer specimens and inhibition of NF-κB activity by a mutant IκBα inhibited PDAC cell tumorigenesis (Fujioka et al., 2003; Wang et al.,

Significance

Pancreatic ductal adenocarcinoma (PDAC) is the fourth most common cause of adult cancer death in the US. The 5-year survival rate has remained 1%–3% for the past 25 years. Each year approximately 42,000 cases of PDAC are diagnosed; over 80% are therapy-resistant locally advanced or metastatic disease, and median survival is less than 6 months. Thus, PDAC remains a challenge in cancer research. To understand mechanisms of pancreatic tumorigenesis, we examined IKK2/β/NF-κB activation and $Kras^{G12D}$ mutation, two of the signature alterations in human PDAC, using genetically engineered mouse models. Our findings establish a pathway linking dual feedforward loops of IL-1α/p62 through which IKK2/β/NF-κB is activated by $Kras^{G12D}$; this suggests therapeutic targets for inhibiting $Kras^{G12D}$ signaling in PDAC.

1999). Thus, these studies demonstrated that IKK2/β/NF-κB has a distinct function in different types of cells. However, it was unclear whether IKK2/β/NF-κB has either prooncogenic or tumor suppressive role in mutant Kras-induced PDAC in mouse models.

Accumulating evidence shows that various signals, including mutant Kras and cytokines activate NF-κB, which, in turn, integrates proinflammatory signals and promote tumorigenesis (Staudt, 2010). For instance, binding of interleukin-1alpha (IL-1α) to its receptor induces K63-linked polyubiquitination of tumor necrosis factor (TNF) receptor-associated factor 6 (TRAF6) and activates transforming growth factor-β-activated kinase 1 (TAK1), which induces activation of IKK2/β, c-Jun N-terminal kinase, and p38 MAPK to activate NF-κB and AP-1 (Skaug et al., 2009; Wang et al., 2001). The turnover of signal-induced K63-polyubiquitination of TRAF6 is prevented by signaling adaptor p62 to prolong IKK2/β and NF-κB activation (Wooten et al., 2005), Furthermore, p62 is an important NF-κB mediator in lung tumorigenesis (Duran et al., 2008), However, the mechanisms that regulate p62 to control IKK2/β activation to the extent of stimulation were unknown. Another report showed that mutant Kras-driven transformation requires TBK1 kinase activation (Barbie et al., 2009). However, the work did not reveal the mechanisms for constitutive NF-κB activation by TBK1 in mutant *Kras*-driven tumor. Studies showed that mutant Kras-associated RAL guanine nucleotide exchange factors promote TBK1 kinase activation via an unknown mechanism, which, in turn, activates c-rel/p50NF-κB, (Chien et al., 2006), and that kinase-inactive TBK1 inhibits TANK-mediated alternative NF-κB activation pathway, but does not block canonical NF-κB activation induced by TNF-α or IL-1 (Pomerantz and Baltimore, 1999). Thus, the mechanisms through which oncogenic Kras activates the canonical NF-κB pathway in PDAC remained unknown.

In the present study, we investigated the role of IKK2/β/NF-κB activation and expression of IL-1α and p62 in *Kras*^{G12D}-induced PDAC development and explored the underlying mechanisms by which IKK2/β/NF-κB is activated by Kras^{G12D}.

RESULTS

Generation of Mutant Mouse Strains with Pancreas-Specific Expression of *Kras*^{G12D} and Inactivation of *IKK2/β* with or without Concurrent *Ink4a/Arf* Deletion

To determine the function of constitutive NF-κB activity in PDAC development, we targeted *IKK2/β* deletion in the pancreas of the *Kras*^{G12D} mice with and without *Ink4a/Arf* inactivation. The mouse strain with floxed *IKK2/β* alleles (*IKK2/β*$^{F/F}$) (Li et al., 2003) is utilized in breeding with the mice that harbors a *Pdx1-Cre* transgene (*Pdx1-Cre*) (Gu et al., 2002) and a latent *Kras*^{G12D} knockin allele (*Kras*$^{LSL-G12D}$) (Hingorani et al., 2003), and those that carry the floxed *Ink4a/ Arf* (*Ink4a/Arf* $^{F/F}$), *Kras*$^{LSL-G12D}$, and *Pdx1-Cre* alleles (Aguirre et al., 2003). Generation of *IKK2/β*$^{F/F}$ genotypes in *Pdx1-Cre;Kras*$^{LSL-G12D}$ and *Pdx1-Cre;Kras*$^{LSL-G12D}$*;Ink4a/Arf*$^{F/F}$ strains are schematically depicted in Figure 1A. *Cre*-mediated excision of the silencing cassette and subsequent recombination generated a single *LoxP* site was detected in the pancreas, but not in other organs such as liver in all of the mouse lines (Figure 1B). Consistent with expression of the mutant *Kras* allele at endogenous level, GTP-bound Ras protein was increased only in protein extracts from the pancreata of the mice carrying *Pdx1-Cre;Kras*$^{LSL-G12D}$ alleles (Figure 1C). The third coding exon-deleted *IKK2/β* alleles were detected in a mosaic pattern in the pancreata of all *Pdx1-Cre;IKK2/β*$^{F/F}$ mice (Figure 1D). As a result, NF-κB DNA binding activities were notably reduced in nuclear extracts from the pancreata of *Pdx1-Cre;Kras*$^{LSL-G12D}$*;IKK2/β*$^{F/F}$ mice, but not in those of *Pdx1-Cre;Kras*$^{LSL-G12D}$ mice (Figures 1E and 1F). Both *p16Ink4a* and *p19Arf* genes were specifically deleted in the pancreata of the mutant mice (Figure 1G). Thus, these results show that the *Pdx1-Cre* transgene concurrently deleted LoxP-containing alleles to target expression of *Kras*^{G12D} and inactivation of *IKK2/β*$^{F/F}$ and/or *Ink4a/Arf*$^{F/F}$ alleles specifically in the pancreata of these mutant mice.

IKK2/β Activity Required for Oncogenic Kras-Induced PanIN and PDAC

To examine the role of IKK2/β in PDAC development, we characterized a cohort of *Pdx1-Cre;Kras*$^{LSL-G12D}$*;IKK2/β*$^{F/F}$ and *Pdx1-Cre;Kras*$^{LSL-G12D}$*;Ink4a/Arf*$^{F/F}$*;IKK2/β*$^{F/F}$ mice and their control littermates. Our findings revealed that these mutant mice did not develop PDAC, unlike their control mice (Figures 2A and 2B). Chi-square analysis showed that the *Pdx1-Cre;Kras*$^{LSL-G12D}$ genotypes with IKK2/β are associated with the observed chronic pancreatis (CP), PanIN lesions, cystic ductal lesion (CDL), and PDAC (Figure 2B), suggesting IKK2/β plays a causal role in PDAC development. Consistent with these results, *Pdx1-Cre;Kras*$^{LSL-G12D}$*;Ink4a/Arf*$^{F/F}$*;IKK2/β*$^{F/F}$ mice remained free of PDAC for over 12 months, whereas the median survival of *Pdx1-Cre;Kras*$^{LSL-G12D}$*;Ink4a/Arf*$^{F/F}$ mice was about 3.5 months, as previously described (Aguirre et al., 2003; Figure 2C).

The littermates of all the mutant mice were born with mendelian frequencies and weight similar to those of wild-type controls. Organs appeared to be formed normally and no phenotypic differences were observed before the age of 2 months in *Pdx1-Cre;Kras*$^{LSL-G12D}$ mice and 6 weeks in *Pdx1-Cre;Kras*$^{LSL-G12D}$*;Ink4a/Arf*$^{F/F}$ mice. No pancreatic ductal lesions or other abnormalities were detected and the expression levels of glucagon, insulin, amylase, CK-19, and staining of duct-specific lectins, Dolichos biflorus agglutinin (DBA) in various *IKK2/β*$^{F/F}$ mice are consistent with those observed in the pancreas of wild-type mice (Figures 2E and 2F; Figure S1 available online). Altogether, the normal histology, marker gene expression, and life span suggest that knockout of IKK2/β in mouse pancreas did not result in abnormal pancreas development in acinar, ductal, and islet of the pancreas or apparent pathological phenotypes.

In *Pdx1-Cre;Kras*$^{LSL-G12D}$*;IKK2/β*$^{F/F}$ mice (Figures 2F and 2G), only 12% (10 of 84) of the mice developed stage 1 PanIN lesions, which consisted primarily of elongated mucinous ductal cells, and no PDAC was observed for over 12 months, whereas 19% (13 of 70) of *Pdx1-Cre;Kras*$^{LSL-G12D}$ mice had PDAC in 8–12 months (Figure 2M), 24% (17 of 70) had CDL during the same time period (Figure 2L), and 27% (19 of 70) had stage 1, 2, or 3 PanIN lesions (Figures 2I–2K) at about 3–6 months. Moreover, most CP was associated with all the PanIN and PDAC, and only 10% of *Pdx1-Cre;Kras*$^{LSL-G12D}$ mice (7 of 70) developed CP without PanIN or PDAC pathological lesions (Figures 2A and 2H). These findings suggest that inactivation of

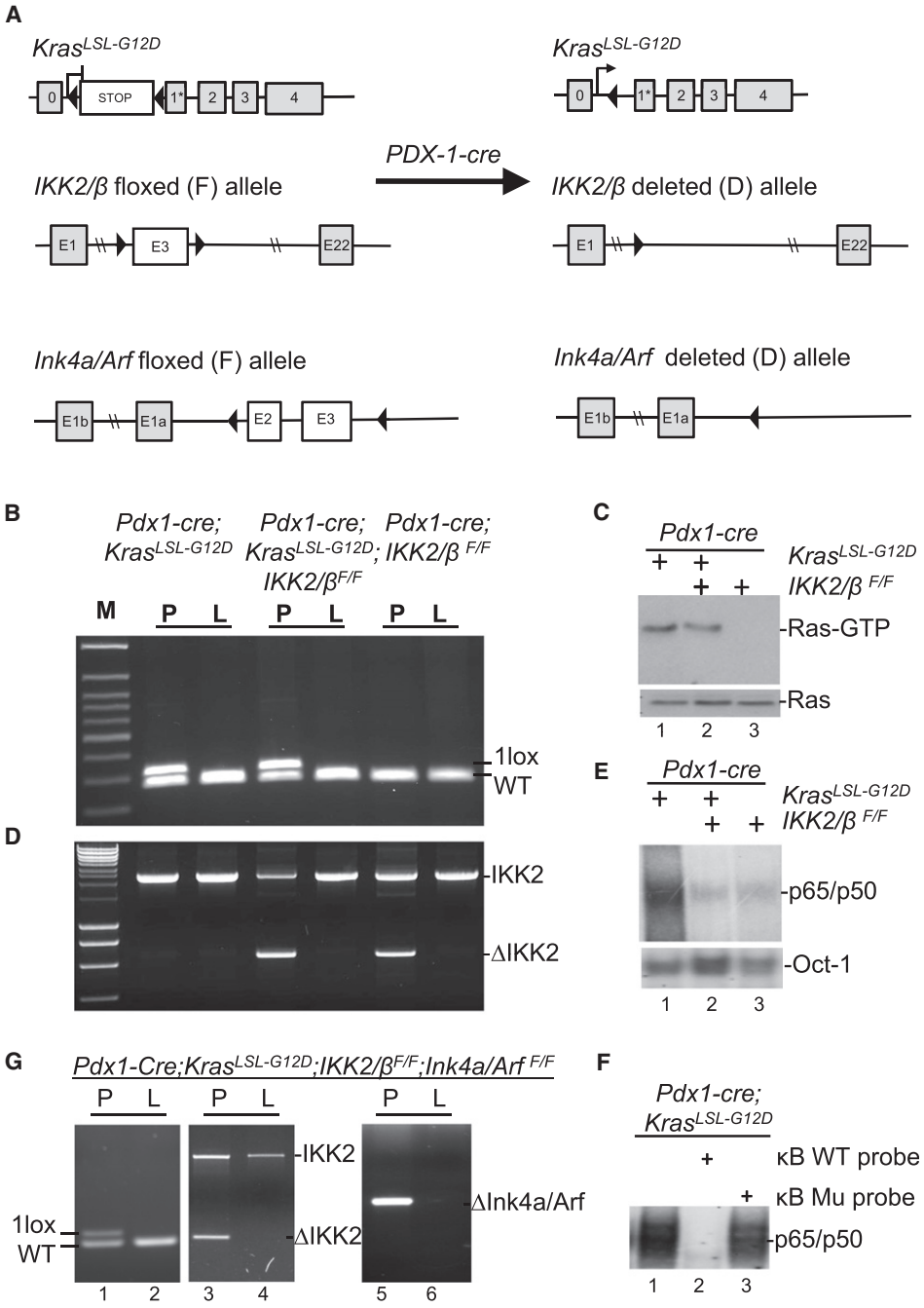

Figure 1. Generation of Mouse Strains with Pancreas-Specific *Kras^{G12D}* Expression and Inactivation of *IKK2/β* with or without Parallel Deletion of *Ink4a/Arf*

(A) Graphic representation of the targeted *Kras$^{LSL-G12D}$*, *IKK2/β*, and *Ink4a/Arf* alleles before and after *Cre*-mediated excision and recombination.

(B) The presence of recombined *Kras^{G12D}* allele in the pancreata (P) but not in the livers (L) of compound mutant mice was revealed by PCR.

(C) Ras-GTP and total Ras levels in whole pancreatic protein extracts of 3-month-old *Pdx1-Cre;Kras$^{LSL-G12D}$*, *Pdx1-Cre;Kras$^{LSL-G12D}$;IKK2/β$^{F/F}$*, and *Pdx1-Cre; IKK2/β$^{F/F}$* mice. Elevated levels of Ras-GTP were observed only in compound mutant mice with *Pdx1-Cre;Kras$^{LSL-G12D}$* alleles.

(D) The recombined *IKK2/β$^{F/F}$* allele was detected only in the pancreata (P), not in the livers (L), of mice carrying *Pdx1-Cre;IKK2/β$^{F/F}$* alleles.

(E) EMSA was performed to determine the levels of NF-κB DNA binding activity in the pancreata carrying *Pdx1-Cre;Kras$^{LSL-G12D}$*, *Pdx1-Cre;Kras$^{LSL-G12D}$;IKK2/β$^{F/F}$*, or *Pdx1-Cre;IKK2/β$^{F/F}$* alleles. Nuclear extracts from mouse pancreata were used in this analysis with a κB probe. Oct-1 probe was used as a loading control.

(F) EMSA was performed with ^{32}P-labeled κB probe in the presence and absence of both unlabeled wild-type (WT) and mutant (Mu) κB probes to determine the specificity of NF-κB DNA binding activity detected in the pancreata of *Pdx1-Cre;Kras$^{LSL-G12D}$* mice as indicated.

(G) Pancreas-specific deletion of *Ink4a/Arf* alleles was confirmed in *Pdx1-Cre; Kras$^{LSL-G12D}$;IKK2/β$^{F/F}$;Ink4a/Arf$^{F/F}$* mice. The presence of the recombined *Kras^{G12D}* allele and the exon 3-deleted *IKK2/β* allele in the pancreata (P) (lane 5) but not in the livers (L) (lane 6) of compound mutant mice was revealed by PCR.

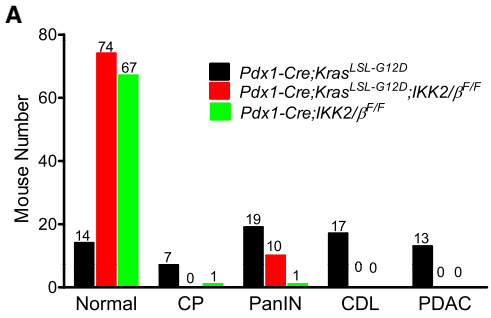

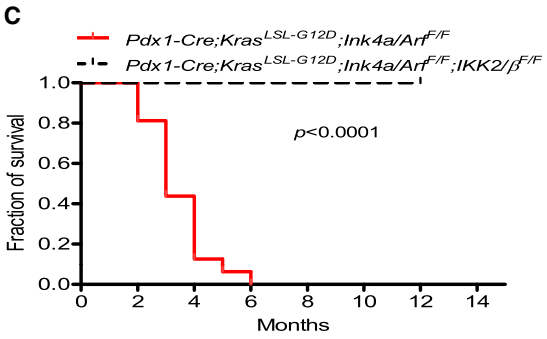

B

Genotype/observed pancreatic lesions	CP	No-CP	PanIN	NO-PanIN	CDL	NO-CDL	PDAC	No-PDAC
Pdx1-cre;Kras$^{LSL-G12D}$	56	14	49	21	30	40	13	57
Pdx1-cre;Kras$^{LSL-G12D}$;IKK2/β$^{F/F}$	10	74	10	74	0	84	0	84
Total mice	66	88	59	95	30	124	13	141
	X^2 = 72.29; p<0.0001		X^2 = 54.53; p<0.0001		X^2 = 44.71; p<0.0001		X^2 = 17.04; p<0.0001	

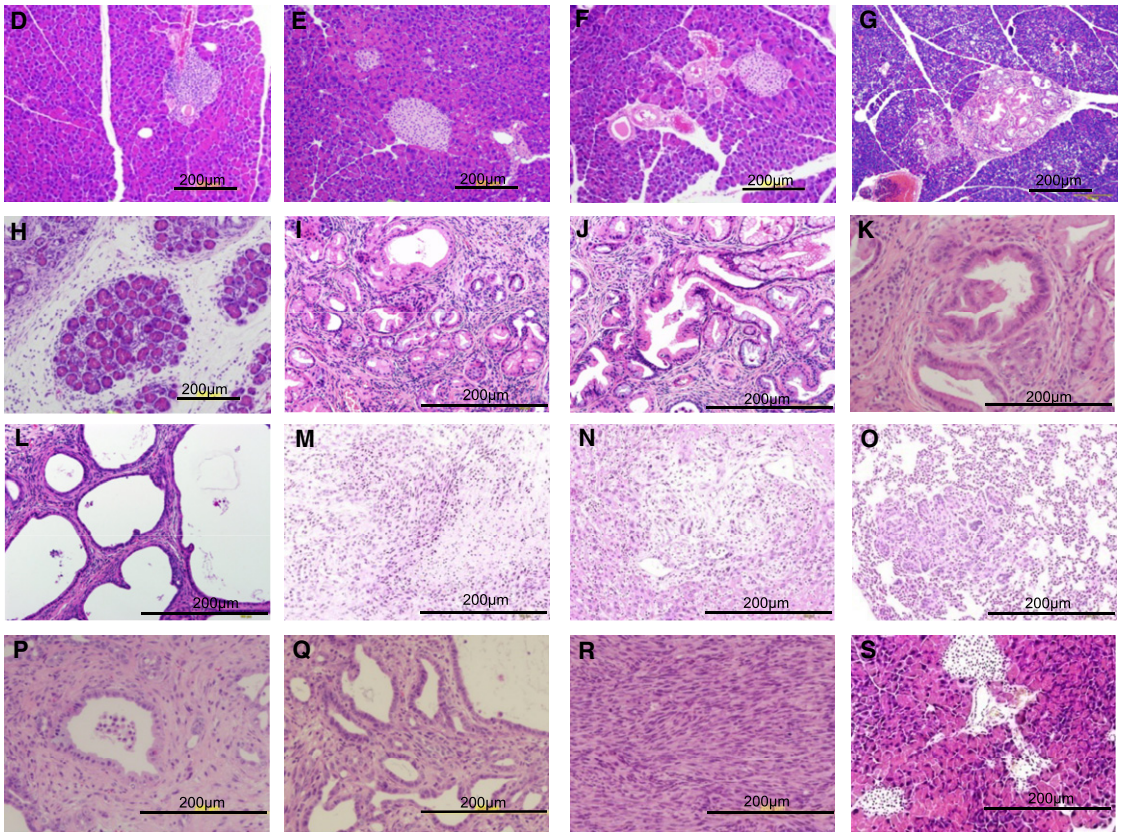

Figure 2. Suppression of Oncogenic *Kras^{G12D}*-Induced Histological Progression of PanIN and PDAC with or without Concurrent Deletion of *Ink4a/Arf* by Inactivation of *IKK2/β*

(A) Numbers of mutant mice that developed PDAC, cystic ductal lesions (CDL), PanIN, or chronic pancreatitis (CP), or remained healthy, in cohorts of *Pdx1-Cre;Kras$^{LSL-G12D}$*, *Pdx1-Cre;Kras$^{LSL-G12D}$;IKK2/$\beta^{F/F}$*, and *Pdx1-Cre;IKK2/$\beta^{F/F}$* mice.

(B) Chi-square analysis of the association between *Pdx1-Cre;Kras$^{LSL-G12D}$* and *Pdx1-Cre;Kras$^{LSL-G12D}$;IKK2/$\beta^{F/F}$*, and the observed phenotypes in (A). Note: CP was found in PanIN, CDL, and PDAC; PanIN was coexisted with CDL and PDAC; and CDL was observed in PDAC.

(C) Kaplan-Meier PDAC-free survival curve for *Pdx1-Cre;Kras$^{LSL-G12D}$;Ink4a/Arf$^{F/F}$* (n = 16) and *Pdx1-Cre;Kras$^{LSL-G12D}$;IKK2/$\beta^{F/F}$;Ink4a/Arf$^{F/F}$* mice (n = 15). According to the approved animal protocol, mice that presented in a moribund state were killed for autopsy.

IKK2/β inhibited PDAC and CP might be a precursor lesion in Kras-induced PDAC.

Serial histological surveys of the pancreas of all the mice are shown in Figures 2D–2S. *Pdx1-Cre;Kras*$^{LSL\text{-}G12D}$ mice had PanIN at 3 months of age and had invasive tumors by 10 months of age, and 3 of 70 had liver or lung metastatic lesions by 8–12 months of age (Figures 2N and 2O). The progressive premalignant lesions with ductal histology and PDAC were observed (Figures 2M–2O and 2R). These PDAC histological lesions and incidences are consistent with those of the mice harboring *Kras*$^{LSL\text{-}G12D}$ or *Kras*$^{LSL\text{-}G12D}$*;Ink4a/Arf*$^{F/F}$ in earlier studies (Aguirre et al., 2003; Tuveson et al., 2004). These results demonstrate that IKK2/β is required for oncogenic Kras-induced PanIN and PDAC, thus establishing a definitive role of IKK2/β in PDAC development in vivo.

Attenuation of Inflammatory and Proliferative Responses by Pancreas-Targeted Inactivation of *IKK2/β*

To determine whether chronic inflammation and proliferative responses were inhibited in the pancreas of *Pdx1-Cre;Kras*$^{LSL\text{-}G12D}$*;IKK2/β*$^{F/F}$ mice, immunohistochemical (IHC) analyses were performed. Levels of proliferation markers CyclinD1, Ki-67, and inflammatory marker COX-2 expression were substantially higher in PanIN and PDAC from *Pdx1-Cre;Kras*$^{LSL\text{-}G12D}$ mice, than in histologically normal pancreas from *Pdx1-Cre;Kras*$^{LSL\text{-}G12D}$*;IKK2/β*$^{F/F}$ mice (Figure 3A). This finding suggests that inactivation of IKK2/β interrupted mutant Kras-stimulated cell proliferation and inflammation.

The observation of CP or proinflammatory responses in *Pdx1-Cre;Kras*$^{LSL\text{-}G12D}$ mice prompted us to examine whether these mutant mice developed lymphocytic infiltration around pancreatic lesions. IHC staining revealed that the infiltrating lymphocytes consisted of CD3-positive T cells, B220-positive B cells, F4/80-positive macrophages, and Ly6g-positive neutrophil (Figure 3B), whereas parallel staining did not reveal significant lymphocytic infiltration in the pancreata of *Pdx1-Cre;Kras*$^{LSL\text{-}G12D}$*;IKK2/β*$^{F/F}$ mice (Figure 3B). This phenotype of lymphocytic infiltration in the pancreata of *Pdx1-Cre;Kras*$^{LSL\text{-}G12D}$ mice has a close resemblance to those reported for various mouse strains with pancreatitis, such as *IκBα*$^{m/m}$ mice defective in IκBα-mediated negative regulation of NF-κB (Peng et al., 2010). So, the absence of hallmarks of cancer-related inflammation in *Pdx1-Cre;Kras*$^{LSL\text{-}G12D}$*;IKK2/β*$^{F/F}$ mice is due to inactivation of IKK2/β. This suggests chronic inflammation is a key factor in promoting PDAC development as observed in mouse models for other cancers (Karin, 2008), and one of the essential roles regulated by IKK2/β in Kras-induced PDAC inception.

Inhibition of Key Proinflammatory Cytokines in the Pancreas of *Pdx1-Cre;Kras*$^{LSL\text{-}G12D}$*;IKK2/β*$^{F/F}$ Mice

To further analyze Kras-induced inflammatory responses, gene expression was profiled and a number of known and previously unknown NF-κB regulated genes were identified by Gene Set Enrichment analyses (GSEA) using gene ontology and NF-κB target gene sets (Figures 4A and 4B; Figures S2A–S2E). Importantly, GSEA of significant gene upregulation in *Pdx1-Cre;Kras*$^{LSL\text{-}G12D}$ revealed that they are strongly associated to positive nodal status, high risk, higher tumor stage, and poor survival in PDAC patients by comparing with 102 PDAC cDNA microarray files (GSE21501) (Figure 4C). Two- and 5-fold enriched expression in *Pdx1-Cre;Kras* $^{LSL\text{-}G12D}$*;IKK2/β*$^{F/F}$ is correlated to low risk (Figures S2A–S2E). These findings further indicate that the significant role of activated IKK2/β in PDAC development.

To further explore the role of IKK2/β in PDAC development, we compared additional gene expression profiles from *Pdx1-Cre;Kras*$^{LSL\text{-}G12D}$ and *Pdx1-Cre;Kras*$^{LSL\text{-}G12D}$*;IKK2/β*$^{F/F}$ mice using Affymetrix arrays. Our results showed that there is a little difference between the expression profiles of several IKK2/β/NF-κB-regulated genes, such as *IL-1α, IL-1β*, and *c-jun* in the histologically normal pancreas from *Pdx1-Cre;Kras*$^{LSL\text{-}G12D}$ and *Pdx1-Cre;Kras*$^{LSL\text{-}G12D}$*;IKK2/β*$^{F/F}$ mice, which might be due to the small fractions of Pdx1-targed cells (Figures S2F and S2G; Table S1). Furthermore, the analysis of the gene expression profiles among the normal pancreas, PanIN, and PDAC from *Pdx1-Cre;Kras*$^{LSL\text{-}G12D}$ mice revealed that these profiles are consistent with those involved in PDAC development as those identified between *Pdx1-Cre;Kras*$^{LSL\text{-}G12D}$ and *Pdx1-Cre;Kras*$^{LSL\text{-}G12D}$*;IKK2/β*$^{F/F}$ mice (Figures 4A–4C; Table S2), and are associated with signaling pathways and cellular functions of genes in tumorigenesis (Figures S2H and S2I). The progressive increases in the expression of several NF-κB regulated genes from low expression in the histological normal pancreas to high expression levels in PanIN and PDAC suggest the involvement of the NF-κB-regulated genes in Kras-induced PDAC development.

Among 20 of the differentially expressed genes with a greater than 10-fold increases in expression in the pancreatic tissues of *Pdx1-Cre;Kras*$^{LSL\text{-}G12D}$ mice (Figure 4A), most of them are cytokines, chemokines, and their receptors, suggesting a role of these molecules in Kras-induced PDAC in vivo. To substantiate the differences in cytokine gene expression between 5- to 12-month-old *Pdx1-Cre;Kras*$^{LSL\text{-}G12D}$ and age-matched *Pdx1-Cre;Kras*$^{LSL\text{-}G12D}$*;IKK2/β*$^{F/F}$ mice, we performed real-time PCR arrays with 84 cytokines and chemokines and validated 9 cytokines with highest expression levels, which includes *IL-1α*, *IL-1β*, and *IL-1 receptor type 2* (Figure 4D; Table S3).

We next investigate the expression of IL-1α and IL-1β, since the expression of both cytokines is among the highest. The levels of IL-1α were significantly elevated in pancreatic tissues and IL-1β levels were slightly higher in serum of *Pdx1-Cre;Kras*$^{LSL\text{-}G12D}$ mice, but not in wild-type, *Pdx1-Cre;IKK2/β*$^{F/F}$, and *Pdx1-Cre;Kras*$^{LSL\text{-}G12D}$*;IKK2/β*$^{F/F}$ mice (Figures 4E and 4F). These results, together with the lymphocytic infiltration, are consistent with chronic inflammation and the role of IKK2/β in cytokine

(D–S) Representative pancreatic histologic views. (D) Normal pancreas from a wild-type mouse. (E) Histologic appearance of normal pancreas from a *Pdx1-Cre;IKK2/β*$^{F/F}$ mouse. (F) Histologic appearance of normal pancreas from a *Pdx1-Cre;Kras*$^{LSL\text{-}G12D}$*;IKK2/β*$^{F/F}$ mouse. (G) A rare PanIN-1 from *Pdx1-Cre;Kras*$^{LSL\text{-}G12D}$*;IKK2/β*$^{F/F}$ mouse. (H–O) *Pdx1-Cre;Kras*$^{LSL\text{-}G12D}$ mice. (H) Chronic pancreatitis (I) PanIN-1. (J) PanIN-2. (K) PanIN-3. (L) Cystic ductal lesion. (M) PDAC. (N) PDAC liver metastasis. (O) PDAC lung metastasis. (P-R) *Pdx1-Cre;Kras*$^{LSL\text{-}G12D}$*;Ink4a/Arf*$^{F/F}$ mice. (P) PanIN. (Q) Cystic ductal lesion. (R) PDAC. (S) Histologic appearance of normal pancreas from a *Pdx1-Cre;Kras*$^{LSL\text{-}G12D}$*;Ink4a/Arf*$^{F/F}$*;IKK2/β*$^{F/F}$ mouse.
See also Figure S1.

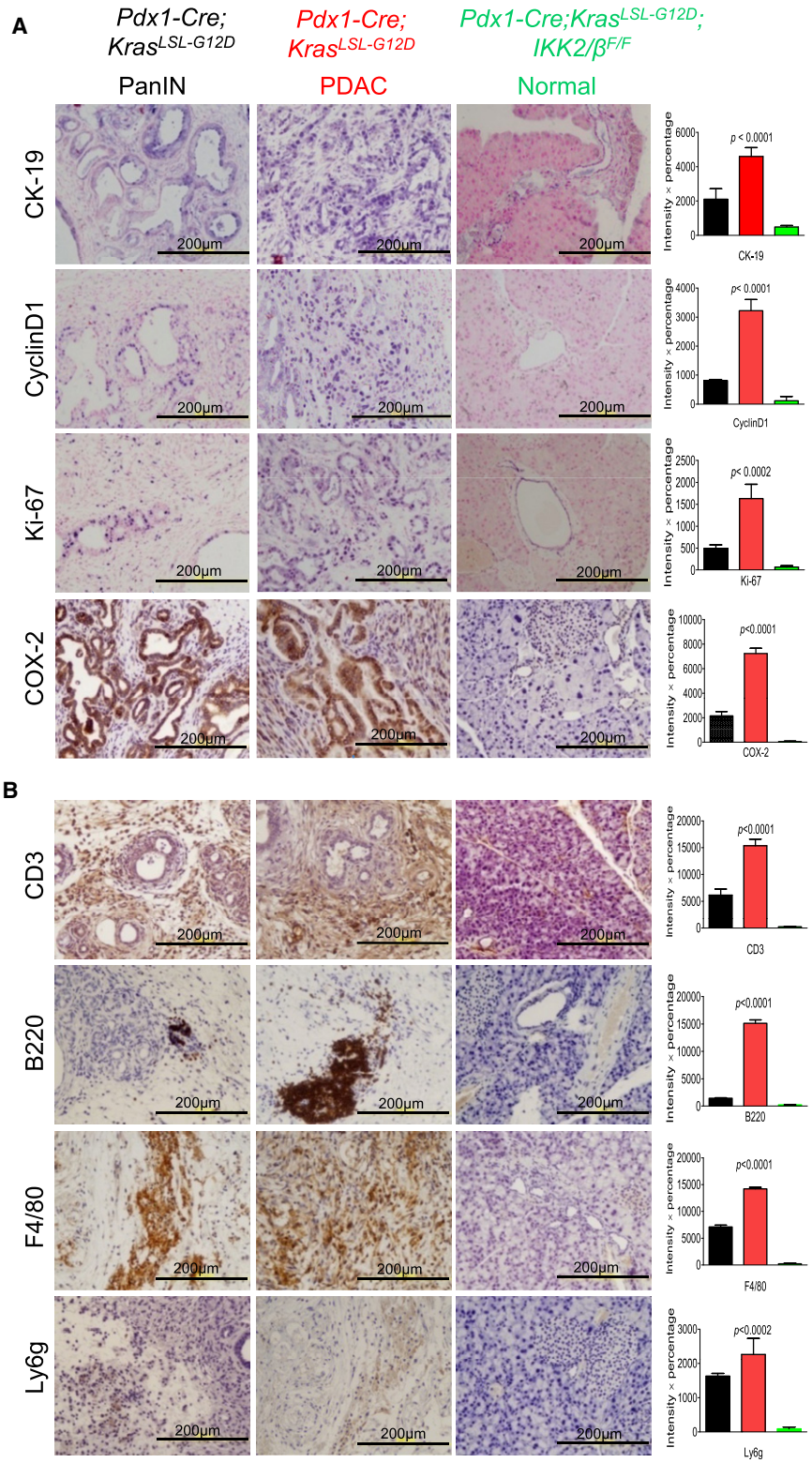

Figure 3. Comparison of the Cell Proliferation, Inflammation, and Immune Responses in the Pancreas between *Pdx1-Cre; Kras$^{LSL-G12D}$;IKK2/β$^{F/F}$* and *Pdx1-Cre; Kras$^{LSL-G12D}$* Mice

(A) Expression of CyclinD1, Ki-67, and COX-2 is elevated in PanIN and PDAC from *Pdx1-Cre; Kras$^{LSL-G12D}$* mice, but not in the normal pancreas of *Pdx1-Cre;Kras$^{LSL-G12D}$;IKK2/β$^{F/F}$* mice. Positive immunostaining for Cytokeratin-19 (CK-19) verifies the ductal phenotype of PanIN lesions, PDAC, and normal duct.

(B) Sections of formalin-fixed PanIN lesions and PDAC from 8-month old *Pdx1-Cre;Kras$^{LSL-G12D}$* and normal duct tissue from *Pdx1-Cre; Kras$^{LSL-G12D}$;IKK2/β$^{F/F}$* mice underwent IHC staining with anti-CD3 antibody as a T cell marker, anti-B220 as a B cell marker, anti-F4/80 as a macrophage marker, and anti-Ly6g as a neutrophil marker. Error bars represent ± standard deviation (SD) from the data of five mice for each of the two genotypes.

expression, which may, in turn, promote a protumorigenic microenvironment. *IL-1α* is an NF-κB target gene and a strong NF-κB inducer (Mori and Prager, 1996; Osborn et al., 1989), but *IL-1α* induction by Kras is previously unknown, suggesting a possible mechanistic link between *IL-1α* expression induced by the Kras^{G12D} and IKK2/β/NF-κB activation.

Downregulation of Expression of IKK2/β/NF-κB Upstream Signaling Molecules by Inactivation of IKK2/β

To elucidate the downstream pathways of mutant Kras that activate IKK2/β, we carried out IHC analysis of PanIN and PDAC to determine the status of inflammation related signaling pathways, including TAK1, p65/RelA, c-Fos, p62, IL-1α, and Rantes (Chemokine [C-C motif] ligand 5). Our results show that levels of c-Fos, TAK1, p62, activated-p65/RelA, IL-1α, and Rantes were substantially higher in PanIN and PDAC from *Pdx1-Cre;Kras$^{LSL-G12D}$* mice than in histologically normal pancreata from *Pdx1-Cre;Kras$^{LSL-G12D}$;IKK2/β$^{F/F}$* mice (Figure 5A). These results suggest that IKK2/β regulates the expression of TAK1, p62, c-Fos, IL-1α, and Rantes as well as NF-κB activation in the diseased pancreas of *Pdx1-Cre;Kras$^{LSL-G12D}$* mice. To determine whether the Kras-induced signaling pathways are also activated in human PDAC, IHC staining was performed using six different PDAC patient specimens with their adjacent normal tissues as controls for a pilot study. The increased levels of IL-1α, TAK1, c-Fos, nuclear p65/RelA recognized by a specific antiactivated p65/RelA antibody (Zabel et al., 1993), p62, and phosphorylated AKT were observed in human PDAC (Figure 5B). Taken together, these results suggest that inactivation of

IKK2/β interrupts oncogenic Kras-mediated pathways regulating expression of c-Fos, IL-1α, TAK1, and p62, and activation of AKT and NF-κB, but how these signaling molecules are regulated by oncogenic Kras through IKK2/β pathways remained largely unclear.

IL-1α Overexpression Correlates with Kras Mutation and NF-κB Activation in Human PDAC Specimens and Poor Survival in PDAC Patients

To determine whether IL-1α overexpression is correlated with mutant Kras in human PDAC specimens, and is induced by Kras^{G12D} in mouse PanIN and PDAC, we sequenced the *Kras* gene from paraffin sections of PDAC specimens from 14 patients who had not undergone neoadjuvant therapies, and from 9 PDAC patient specimens derived from the orthotopic xenograft mouse model implanted with freshly isolated patient pancreatic cancer for excluding normal human stromal cells (Kim et al., 2009). Ninety-three percent (13 of 14) Kras gene from PDAC paraffin sections has substitutional mutation at codon 12, from GGT (Gly) to GAT (Asp). 71% (5 of 7) Kras mutations identified in human PDAC tissue xenograft also have aspartic acid at codon 12, whereeas 29% (2 of 7) were changed to GTT (valine). The results of IL-1α expression, analyzed by chi-square test, showed that the presence of mutated *Kras* gene positively correlated with IL-1α overexpression in PDAC patient specimens (Figure 6A). Further study of IL-1α expression using human PDAC tissue microarray (TMA) demonstrated that IL-1α overexpression was found in most of the human PDAC tissues. Kaplan-Meier survival analysis indicated that high levels of IL-1α expression are associated with poor survival in PDAC patients ($p = 0.016$, log rank test) (Figure 6B).

To determine the association between NF-κB activity and expression levels of IL-1α in human PDAC for validating the relevance of the observations in *Pdx1-Cre;Kras$^{LSL-G12D}$* and *Pdx1-Cre; Kras$^{LSL-G12D}$;IKK2/β$^{F/F}$* mice, IHC staining for p65 and IL-1α in patient PDAC TMA was performed. 42 of 131 (32%) human PDAC samples showed very strong IL-1α staining and 47 (36%) had extremely intense staining for NF-κB activities (Figure 6C). Data analysis of these by Spearman's rank order correlation showed the positive correlation between NF-κB activities and expression levels of IL-1α (Figure 6D). Altogether, the results suggest that the oncogenic Kras-mediated pathway induced IL-1α overexpression, which triggered NF-κB activation. To determine how early activated NF-κB can be detected during PDAC development, we analyzed the staining of p65/RelA in our pancreatic TMA, and the results show 49% (20/41) positive staining in PanIN stage (Figures S3A and S3B), suggest that NF-κB activation is one of the earliest molecular alterations observed in the development of pancreatic cancer.

To determine whether expression of IL-1α and p62 was induced in by Kras^{G12D}, we examined the levels of IL-1α and p62 expression in human PDAC cell lines MDAPanc-28, AsPc-1, and in immortalized human pancreatic ductal cell lines HPDE and HPNE, with or without stable expression of mutant Kras. Expression of both IL-1α and p62 was elevated in MDAPanc-28 and AsPc-1 cells (Figure 6E) and in HPDE and HPNE cells expressing oncogenic Kras (Figure 6F). The expression of c-Fos and activation of Jun N-terminal kinase (JNK) was also induced in mutant *Kras* HPNE cells (Figure S3C).

To determine whether oncogenic Kras-induced AP-1 activity played a major role in the *IL-1α* and *p62* expression, we performed *IL-1α* and *p62* promoter analysis in mPDAC cells, an early passage mouse PDAC cell lines established from the PDAC of *Pdx1-Cre;Kras$^{LSL-G12D}$* mice. Our reporter gene assays show that *IL-1α* promoter with mutated *AP-1* sites had no responses, whereas activity of *IL-1α* promoter with wild-type *AP-1* sites was strongly inhibited by expression of a mutant of *ras* (RasN17), *c-fos* (*FosDN*), and *IκBα* (*IκBαM*), as well as kinase-dead *raf* and *jnk* (Figure 6G). Similarly, *p62* promoter was strongly inhibited by expression of *FosDN* and *IκBαM* (Figure 6H). The results showed that *IL-1α* and *p62* promoters in mPDAC cells were regulated by Kras through AP-1 and NF-κB transcription factors.

Identifying Feedforward Mechanisms that Sustain Constitutive NF-κB Activation in Oncogenic Kras^{G12D}-Induced PDAC

To determine whether IL-1α serves a mechanistic link between Kras^{G12D} and NF-κB activation, we utilized two human PDAC cell lines and two early passage mouse PDAC cell lines, mPDAC-1 and mPDAC-2, which were established from PDAC of *Pdx1-Cre;Kras$^{LSL-G12D}$* mice. These cells were treated with anti-IL-1α and anti-IL-1β neutralizing antibodies for 0, 4, and 8 hr and the nuclear extracts were analyzed. The results showed that anti-IL-1α, but not anti-IL-1β, neutralizing antibodies blocked constitutive NF-κB activation (Figures 7A and 7B). These findings suggest that secreted IL-1α from these cells activates NF-κB through autocrine mechanism.

Although p62 was induced by Kras to trigger IKK2/β activation in lung cancer cells (Duran et al., 2008), the mechanisms are still lacking. To determine whether and how p62 is involved in Kras^{G12D}-induced IKK2/β/NF-κB activation, we stimulated p62-knockdown cells and control cells expressing a puromycin resistant vector and scrambled shRNA with IL-1α for 0, 0.5, 2, or 8 hr and then analyzed NF-κB activity by EMSA (Figures 7C and 7D). The results revealed that constitutive NF-κB activity was decreased in both mPDAC and AsPc-1 *p62* knockdown cells (Figure 7D; Figures S4A and S4B). Interestingly, NF-κB activity was induced to the same peak level by IL-1α at 0.5 hr stimulation in the control and *p62* knockdown cells, remained at the same level at the end of 2 hr stimulation, and was inhibited at the end of 8 hr of IL-1α stimulation for the *p62* knockdown cells compared with their control cells (Figure 7D; Figures S4A and S4B). These findings suggest that p62 expression is dispensable for IL-1α-induced NF-κB activation at the early phase (Figure 7D, lanes 4–9; Figures S4A and S4B), but is required for IL-1α-induced long-term NF-κB activation (Figure 7D, lanes 10–12; Figures S4A and S4B). Since p62 expression was substantially increased in PanIN and PDAC from *Pdx1-Cre;Kras$^{LSL-G12D}$* mice in comparison to those from histologically normal pancreata from *Pdx1-Cre;Kras$^{LSL-G12D}$;IKK2/β$^{F/F}$* mice (Figures 5A and 5B), it is possible that *p62* is one of the previous unknown downstream target genes regulated by NF-κB. To test this possibility, we showed p62 expression was substantially inhibited in MDAPanc-28 and AsPc-1 cells by expressing *IκBαM* in comparison with their control cells (Figure 7E). Our results also show that both *p62* mRNA and protein levels were increased by IL-1α stimulation and reduced by the

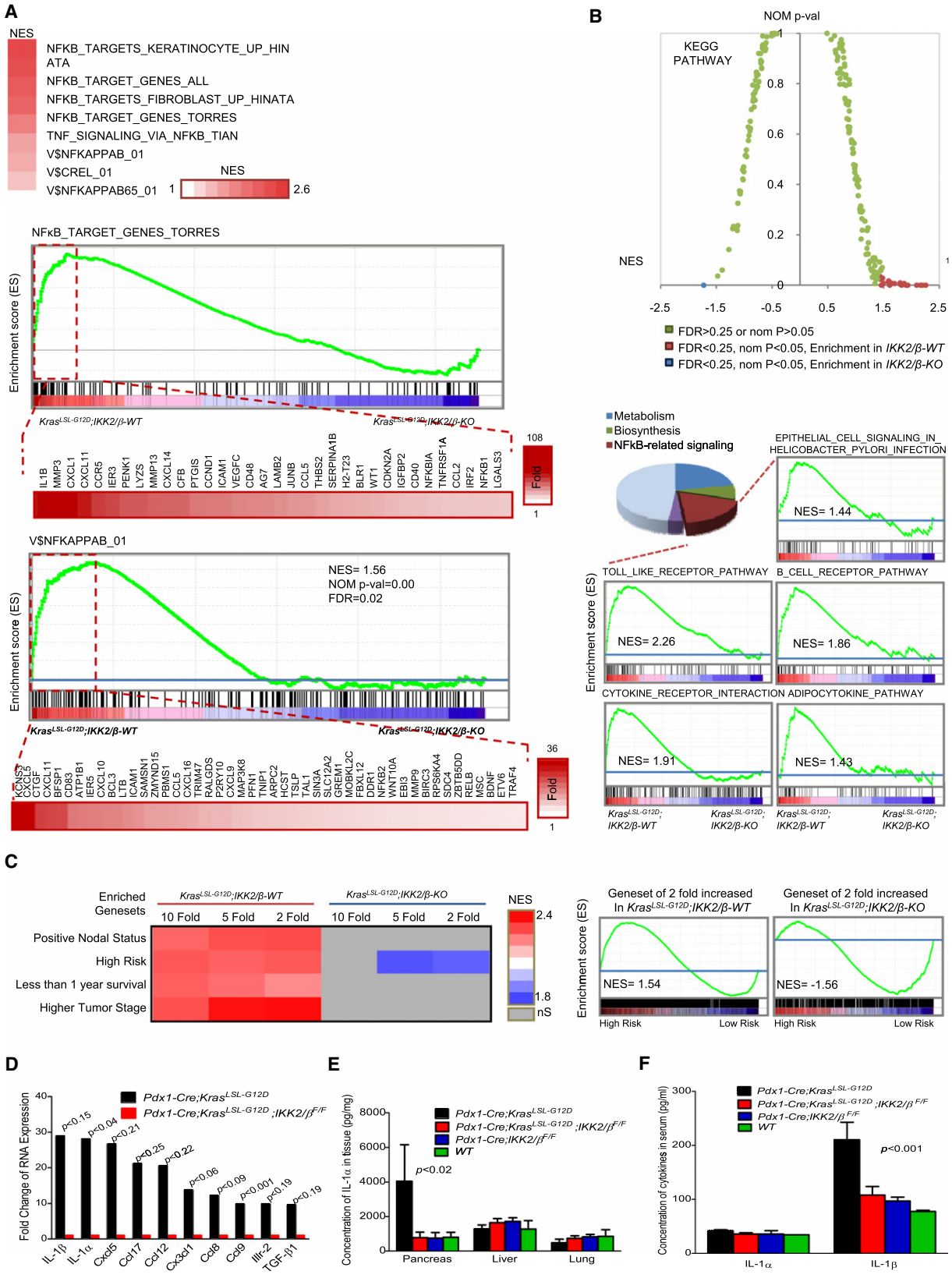
A
NES
NFKB_TARGETS_KERATINOCYTE_UP_HINATA
NFKB_TARGET_GENES_ALL
NFKB_TARGETS_FIBROBLAST_UP_HINATA
NFKB_TARGET_GENES_TORRES
TNF_SIGNALING_VIA_NFKB_TIAN
V$NFKAPPAB_01
V$CREL_01
V$NFKAPPAB65_01
NES
1
2.6
NFκB_TARGET_GENES_TORRES
Enrichment score (ES)
Kras$^{LSL-G12D}$;IKK2/β-WT
Kras$^{LSL-G12D}$;IKK2/β-KO
IL1B MMP3 CXCL1 CXCL11 CCR5 IER3 PENK1 LYZS MMP13 CXCL14 CFB PTGIS CCND1 ICAM1 VEGFC CD48 AG7 LAMB2 JUNB CCL5 THBS2 SERPINA1B H2-T23 BLR1 WT1 CDKN2A IGFBP2 CD40 NFKBIA TNFRSF1A CCL2 IRF2 NFKB1 LGALS3
108
Fold
1
V$NFKAPPAB_01
NES= 1.56
NOM p-val=0.00
FDR=0.02
KCNS3 CCL5 CTGF CXCL11 BFSP1 CD83 ATP1B1 IER5 CXCL10 BCL3 LTB ICAM1 SAMSN1 ZMYND15 PBMS1 CCL5 CXCL16 TRIM47 RALGDS P2RY10 CXCL9 MAP3K8 PFN1 TNIP1 ARPC2 HCST TSLP TAL1 SIN3A SLC12A2 GREM1 MOBKL2C FBXL12 DDR1 NFKB2 WNT10A EBI3 MMP9 BIRC3 RPS6KA4 SDC4 ZBTB5DD RELB MSC BDNF ETV6 TRAF4
36
Fold
1
B
NOM p-val
KEGG PATHWAY
NES
1
0.8
0.6
0.4
0.2
0
-2.5 -1.5 -0.5 0.5 1.5 2.5
FDR>0.25 or nom P>0.05
FDR<0.25, nom P<0.05, Enrichment in IKK2/β-WT
FDR<0.25, nom P<0.05, Enrichment in IKK2/β-KO
Metabolism
Biosynthesis
NFkB-related signaling
EPITHELIAL_CELL_SIGNALING_IN_HELICOBACTER_PYLORI_INFECTION
NES= 1.44
TOLL_LIKE_RECEPTOR_PATHWAY
NES= 2.26
B_CELL_RECEPTOR_PATHWAY
NES= 1.86
CYTOKINE_RECEPTOR_INTERACTION
NES= 1.91
ADIPOCYTOKINE_PATHWAY
NES= 1.43
Enrichment score (ES)
Kras$^{LSL-G12D}$; IKK2/β-WT
Kras$^{LSL-G12D}$; IKK2/β-KO
C
Enriched Genesets
Kras$^{LSL-G12D}$;IKK2/β-WT
Kras$^{LSL-G12D}$;IKK2/β-KO
10 Fold
5 Fold
2 Fold
10 Fold
5 Fold
2 Fold
Positive Nodal Status
High Risk
Less than 1 year survival
Higher Tumor Stage
NES
2.4
1.8
nS
Geneset of 2 fold increased In Kras$^{LSL-G12D}$;IKK2/β-WT
Geneset of 2 fold increased In Kras$^{LSL-G12D}$;IKK2/β-KO
Enrichment score (ES)
NES= 1.54
NES= -1.56
High Risk
Low Risk
High Risk
Low Risk
D
Fold Change of RNA Expression
Pdx1-Cre;Kras$^{LSL-G12D}$
Pdx1-Cre;Kras$^{LSL-G12D}$;IKK2/β$^{F/F}$
p<0.15
p<0.04
p<0.21
p<0.25
p<0.22
p<0.06
p<0.09
p<0.001
p<0.19
p<0.19
IL-1β IL-1α Cxcl5 Ccl17 Ccl12 Cx3cl1 Ccl8 Ccl9 Il1r-2 TGF-β1
E
Concentration of IL-1α in tissue (pg/mg)
Pdx1-Cre;Kras$^{LSL-G12D}$
Pdx1-Cre;Kras$^{LSL-G12D}$;IKK2/β$^{F/F}$
Pdx1-Cre;IKK2/β$^{F/F}$
WT
p<0.02
Pancreas
Liver
Lung
F
Concentration of cytokines in serum (pg/ml)
Pdx1-Cre;Kras$^{LSL-G12D}$
Pdx1-Cre;Kras$^{LSL-G12D}$;IKK2/β$^{F/F}$
Pdx1-Cre;IKK2/β$^{F/F}$
WT
p<0.001
IL-1α
IL-1β

anti-IL-1α neutralizing antibody and by silencing *IKK2/β* expression in MDAPanc-28, AsPc-1, mPDAC-1, and mPDAC-2 cells (Figures 7F–7H; Figure S4C), demonstrating that *p62* expression is regulated by NF-κB activity. To further demonstrate the regulation of *p62* expression by NF-κB, we identified two κB and three AP-1 binding sites in both 3.0 kb human and mouse *p62* promoters, which have extensive DNA sequence similarity (Figure 7I). The results from ChIP assays revealed that NF-κB BS2 and AP-1 BS3 sites showed higher binding activity upon IL-1α stimulation in mPDAC-1 cells (Figure 7J). EMSA showed that NF-κB BS2 site displayed the most κB binding activity, consistent with the results of ChIP assay, whereas the three AP-1 binding sites showed similar binding activity in mPDAC-1 cells (Figure S4D). The luciferase reporter gene assays, using different *p62* promoter constructs with and without mutated AP-1 or κB binding sites and controls, showed that *p62* expression is mainly regulated by NF-κB activity through NF-κB BS2 site and is also mediated by the three AP-1 sites in mPDAC cells, suggesting that *p62* is an NF-κB and AP-1 downstream target gene (Figure 7K). Furthermore, our results showed that NF-κB was activated in the *Kras^{G12D}* PDAC model in the presence of wild-type *p53* function (Figures S4E and S4F), and FOXO3a was stabilized and TSC1 was activated, whereas p70/S6K was not phosphorylated in *IKK2/β* knockdown cells (Figures S4G and S4H), suggesting that both TSC1 and FOXO3a pathways is also involved in Kras-induced PDAC development.

To demonstrated the role of IL-1α and p62 in mutant Kras-driven cancer cells, we knocked down *IL-1α* and *p62* expression in mPDAC cells and in LKP-13, a lung adenocarcinoma cell line derived from *Kras^{G12D}*(LA1) mice (Wislez et al., 2005; Figure 8A; Figures S5A and S5B), and showed significant reduction of tumorigenic potential in the *IL-1α* and *p62* knocked down cancer cells in orthotopic xenograft mouse and subcutaneous xenograft mouse models (Figures 8B-D). Knocking down *TRAF6*, which is essential for IKK2/β and JNK activation in the IL-1α and TLR pathways (Lomaga et al., 1999; Naito et al., 1999), decreased NF-κB activation in both mPDAC cells expressing *Kras^{G12D}* (Figures 8E–8G). Taken together, these results suggest that IL-1α and p62 play a key role in oncogenic Kras-induced tumors. Knocking down of *c-fos* expression inhibited *IL-1α* and *p62* expression and NF-κB activation (Figures 8H–8L). These results suggest that AP-1 activated by oncogenic Kras induced and sustained activation of RelA/p50 in PDAC development.

As illustrated in Figure 8M, our findings suggest a mechanism by which oncogenic Kras signaling pathway induced constitutive activation of NF-κB in PDAC development.

DISCUSSION

We have unequivocally demonstrated that the requirement of NF-κB pathway for PDAC development and the mechanism through which constitutive NF-κB activation and inflammatory responses were induced by oncogenic Kras during PDAC initiation. These findings suggest that the *primum movens* responsible for cancer-related inflammatory responses and the development of PanIN and PDAC is the mutant Kras-initiated constitutive activation of NF-κB. Importantly, our results suggest that mutant Kras may induce intrinsic inflammatory responses that promote a protumorigenic microenvironment through expressing inflammatory mediators such as chemokines and cytokines in tumor tissues, recruiting inflammatory cells, and inducing angiogenesis and tissue repair similar to those observed in hereditary pancreatitis, which has been firmly linked to the development of PDAC (Brentnall et al., 1999; Lowenfels et al., 1997). Thus, our findings further suggest that sporadic PDAC is also induced through a chronic inflammatory mechanism similar to those observed in hereditary pancreatitis related PDAC cases.

Although studies have demonstrated that mutant Ras was shown to activate NF-κB in several types of tumors in mouse models (Bassères et al., 2010; Meylan et al., 2009; Yang et al., 2010). Signaling pathways leading to the constitutive NF-κB activity in cancer cells were not clear at all. Duran et al. (2008) showed that mutant Ras induced p62 expression through AP-1 to activate IKK2/β and NF-κB. However, the requirement for p62 in NF-κB activation is not completely understood considering the reported function of p62 as an adaptor for regulating E3 ubiquitin-protein ligase TRAF6 and deubiquitination enzyme CYLD to balance the turnover of K63-polyubiquitination (Sanz et al., 2000; Wooten et al., 2005). Our results clearly demonstrated that p62 expression is not required for rapid and early NF-κB activation induced by IL-1α, but it is essential for

Figure 4. Gene Ontology and Gene Set Enrichment Analyses between Pancreata from *Pdx1-Cre;Kras$^{LSL-G12D}$* and *Pdx1-Cre;Kras$^{LSL-G12D}$;IKK2/β$^{F/F}$* Mice and Profiling Cytokine Expression

(A) Enriched expression of NF-κB downstream target gene sets in *Pdx1-Cre;*Kras$^{LSL-G12D}$*;IKK2/β^{WT}* compared to *Pdx1-Cre;Kras$^{LSL-G12D}$;IKK2/β$^{F/F}$*. The heat map represents top enriched genes in *Pdx1-Cre;*Kras$^{LSL-G12D}$*;IKK2/β^{WT}*. NES, normalized enrichment score; NOM p value, nominal p value; FDR, false discovery rate q value. (red, high expression; blue, low expression).

(B) GSEA analyses identify the enriched gene sets expressed either in *Pdx1-Cre; Kras$^{LSL-G12D}$;IKK2/β^{WT}* or *Pdx1-Cre;Kras$^{LSL-G12D}$;IKK2/β$^{F/F}$* using 198 KEGG pathway gene sets. One gene set are enrich in *Pdx1-Cre;Kras$^{LSL-G12D}$;IKK2/β^{WT}* and twenty seven gene sets are enriched in *Pdx1-Cre;Kras$^{LSL-G12D}$;IKK2/β$^{F/F}$*. Five NF-κB pathway-related gene sets are noteworthy enriched in *Pdx1-Cre;Kras$^{LSL-G12D}$; IKK2/β^{WT}*. Enriched gene sets were selected based on statistical significance (FDR q value < 0.25 and normalized p value < 0.05).

(C) GSEA analyses of significant gene upregulation in *Pdx1-Cre;Kras$^{LSL-G12D}$* revealed that they are strongly correlated to positive nodal status, high risk, higher tumor stage, and poor survival in PDAC patients by using 102 PDAC cDNA microarray data (GSE21501). Two- and 5-fold enriched expression in *Pdx1-Cre;Kras$^{LSL-G12D}$; IKK2/β$^{F/F}$* is correlated to low risk. ns, not significant (FDR q value > 0.25 and/or normalized p value > 0.05).

(D) Analysis of differential cytokine gene expression between pancreatic cancer and normal pancreas (from 5- to 12-month-old *Pdx1-Cre;Kras$^{LSL-G12D}$* mice and age-matched *Pdx1-Cre;Kras$^{LSL-G12D}$;IKK2/β$^{F/F}$* mice) by real-time PCR arrays.

(E) Determination of IL-1α expression levels in pancreas, liver, and lung from *Pdx1-Cre;Kras$^{LSL-G12D}$*, *Pdx1-Cre;Kras$^{LSL-G12D}$;IKK2/β$^{F/F}$*, *Pdx1-Cre;IKK2/β$^{F/F}$*, and *wild-type* (*WT*) mice.

(F) Evaluation of IL-1α and IL-1β expression levels in sera from *Pdx1-Cre;Kras$^{LSL-G12D}$*, *Pdx1-Cre;Kras$^{LSL-G12D}$;IKK2/β$^{F/F}$*, *Pdx1-Cre;IKK2/β$^{F/F}$*, and *wild-type* (*WT*) mice. Error bars represent ±SD of the data from three mice in each genotype as indicated. See also Figure S2 and Tables S1–S3.

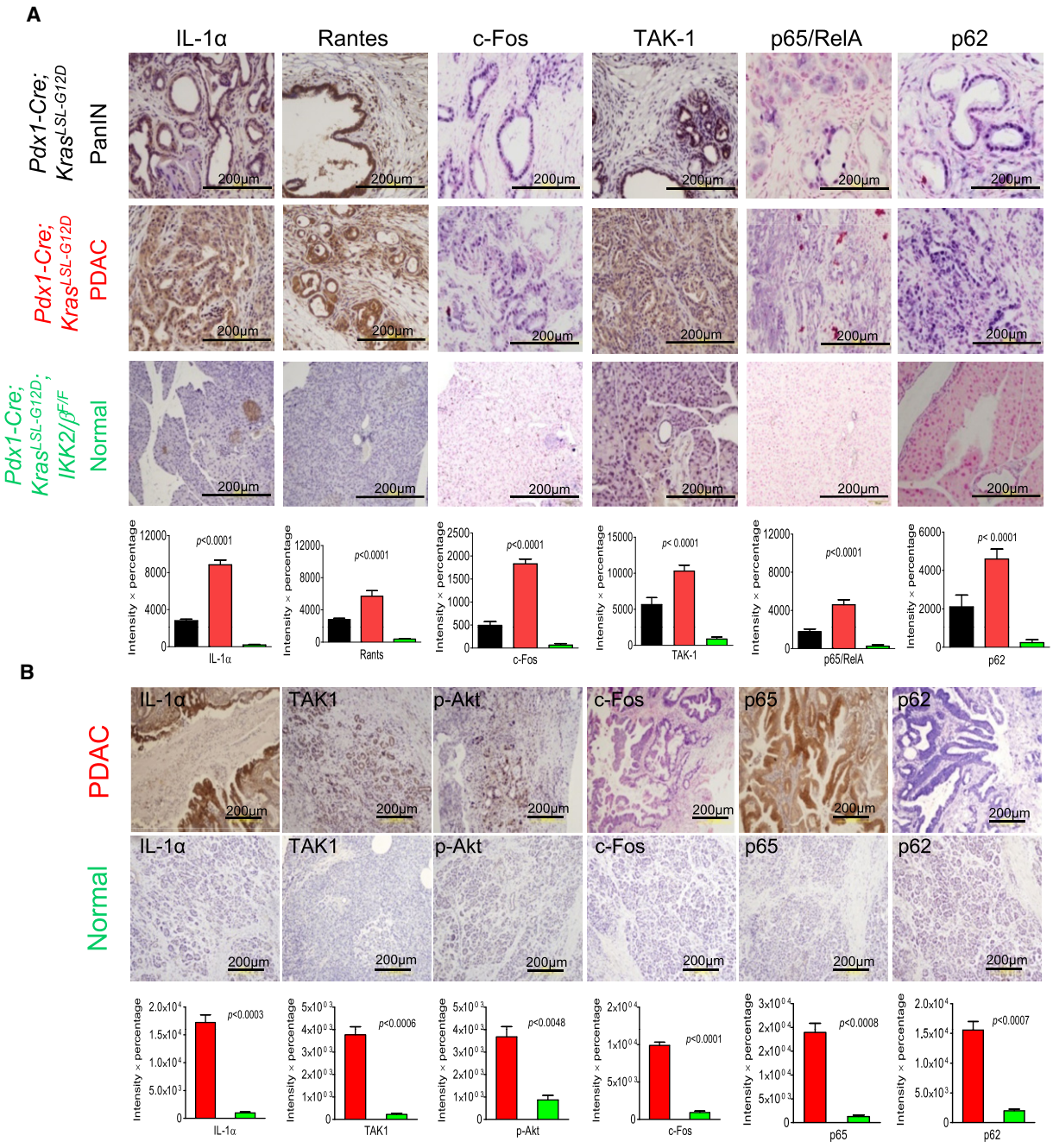

Figure 5. Analysis of Signaling Pathways in PanIN, PDAC, and Histologically Normal Pancreas from Compound Mutant Mice and Human PDAC Patients

(A) Immunohistochemical analysis with anti-IL-1α, anti-Rantes (Chemokine [C-C motif] ligand 5), anti-c-Fos, anti-TAK1, anti-p62, and anti-p65 antibodies in sections of formalin-fixed PanIN lesions and PDAC from *Pdx1-Cre;*$Kras^{LSL-G12D}$ mice, and of normal duct tissues from *Pdx1-Cre;*$Kras^{LSL-G12D}$*;IKK2/*$\beta^{F/F}$ mice. Error bars represent ±SD from the data of five mice for each of the three genotypes.

(B) Immunohistochemical staining for IL-1α, TAK1, pAKT, c-Fos, p65, and p62 in sections of formalin-fixed human PDAC and adjacent histologically normal pancreatic tissues. Error bars represent ±SD from six human PDAC specimens.

constitutive NF-κB activation (Figure 7D; Figures S4A and S4B), which is consistent with the function of p62 as an adaptor for regulating the turnover of K63-polyubiquitinated proteins, including TRAF6, to maintain IKK2/β and NF-κB activation (Sanz et al., 2000; Wooten et al., 2005). Our results show that expression of *p62* is induced by NF-κB activation during IL-1α stimulation of mouse and human PDAC cell lines (Figures 7E–7J), suggesting the existence of an autoregulatory loop whereby NF-κB regulates *p62* expression, which, in turn, extends NF-κB activation.

A

PDAC Patient Specimens	*Kras* Status		IL-1α Expression	% of IL-1α Positive Specimens
PDAC Paraffin Sections	Lymphocyte DDA: N.D.	Wide-type in PDAC DNA (1)	High: 0	0
			Low: 1	100%
		Mutant in PDAC DNA (13)	High: 9	69.2%
			Low: 4	30.8%
PDAC Xenograft Tissues	Lymphocyte DNA: Wide-type	Wide-type in PDAC DNA (2)	High: 0	0
			Low: 2	100%
		Mutant in PDAC DNA (7)	High: 5	71.4%
			Low: 2	28.6%

IL-1α expression vs Kras Mutant: $p<0.05$, $X^2=5.37$

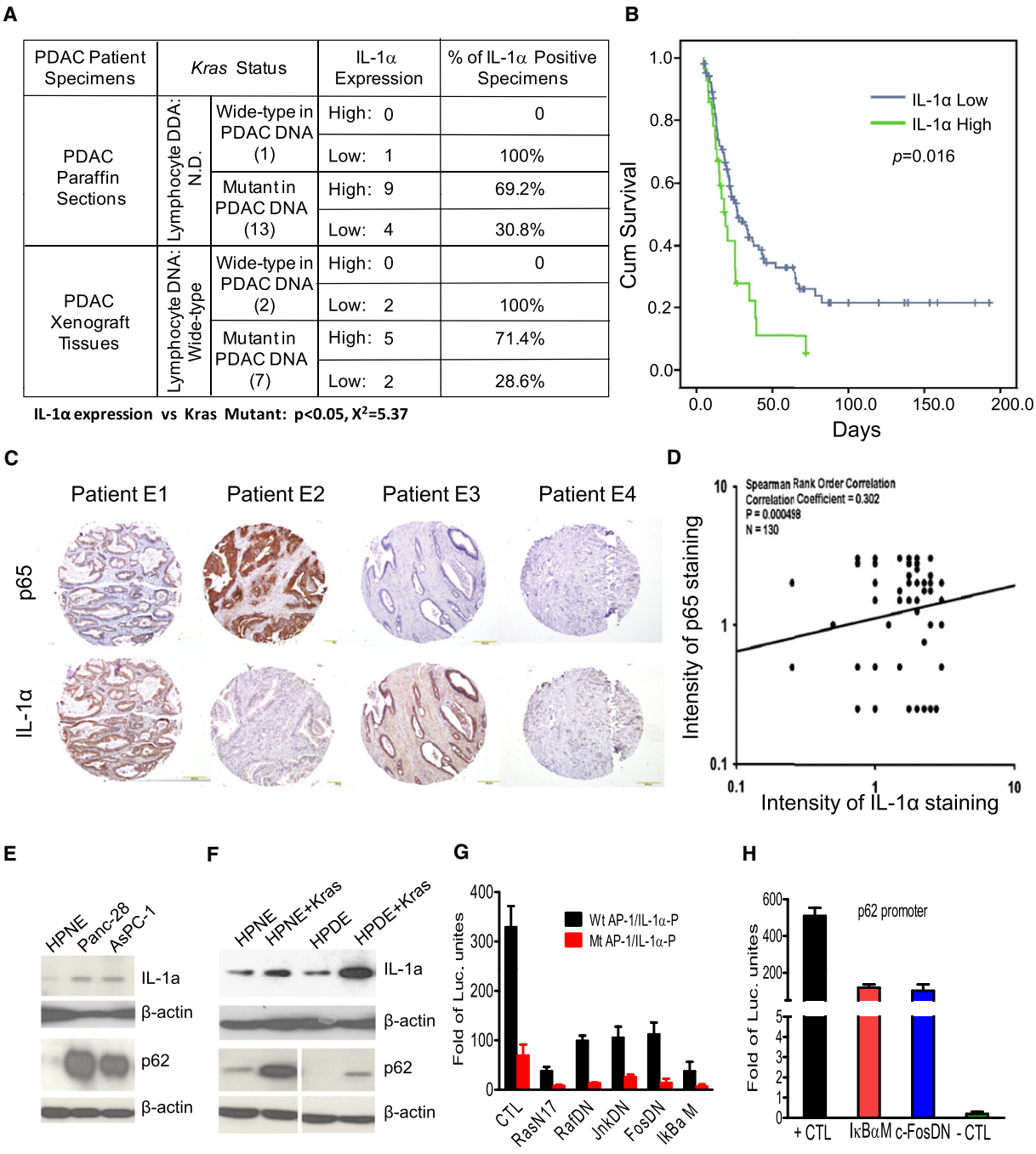

Figure 6. Clinical Correlations among Mutant *Kras*, IL-α Overexpression, and NF-κB Activation in Human PDAC

(A) The percentages of IL-1α positivity in PDAC tissues carrying a mutant *Kras* gene. Chi-square test was used to demonstrate the positive correlation between overexpression of IL-1α and the presence of a mutant *Kras* in PDAC tissues.

(B) Kaplan-Meier survival analysis of PDAC patients with and without high levels of IL-1α expression using TMA.

(C) Immunohistochemical staining for p65 and IL-1α in human PDAC tissue microarrays. Representative IHC stainings are shown, with four combinations of immunostaining patterns, E1: p65 high, IL-1α high; E2: p65 high, IL-1α low; E3: p65 low, IL-1α high; E4: p65 low, IL-1α low.

(D) Scores of activated NF-κB are plotted against those of IL-1α overexpression. Spearman's rank order correlation was used to demonstrate the positive correlation between NF-κB activity and expression levels of IL-1α in TMA.

(E) Western blot analysis showing IL-1α and p62 overexpression in pancreatic cancer cell lines MDAPanc-28 and AsPc-1.

(F) Western blot analysis of IL-1α and p62 expression in hTERT-immortalized human pancreatic ductal HPNE and HPDE cell lines.

(G) Reporter gene assay for analyzing *IL-1α* promoter regulation by Kras, AP-1, and NF-κB pathways using mPDAC cells.

(H) Reporter gene assay for analyzing the regulation of *p62* promoter by AP-1 and NF-κB pathways using mPDAC cells. Error bars represent ±SD from three independent experiments. See also Figure S3.

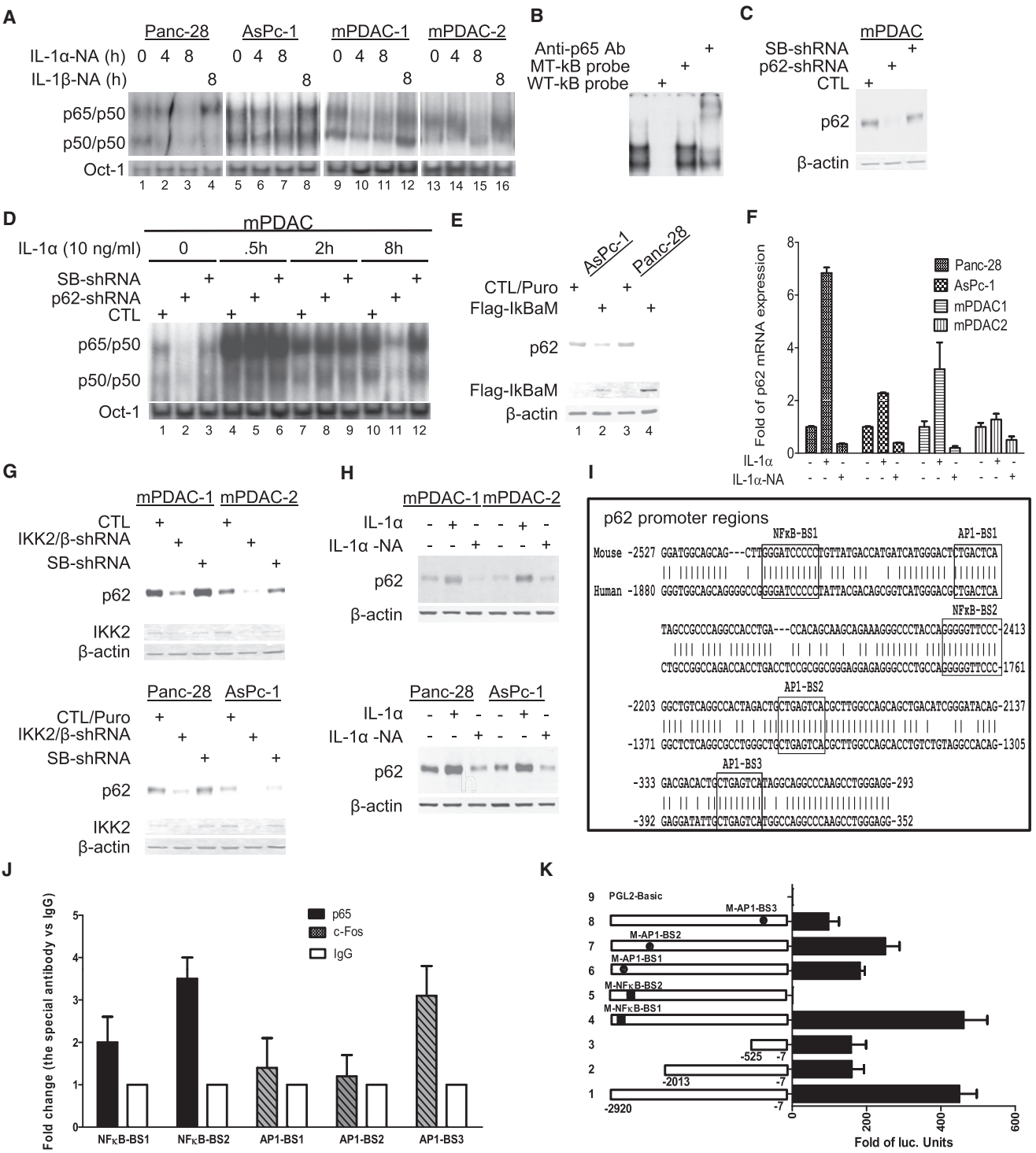

Figure 7. Elucidation of Feedforward Signaling Pathways that Sustain Constitutive NF-κB Activation in Oncogenic *Kras^{G12D}*-Induced PDAC

(A) Nuclear extracts of human PDAC cell lines MDAPanc-28 and AsPc-1 and mouse PDAC cell lines mPDAC-1 and mPDAC-2 (derived from *Pdx1-Cre; Kras$^{LSL-G12D}$*), treated with anti-IL-1α neutralizing antibody (2 μg/ml) for 0, 4, or 8 hr or with anti-IL-1β neutralizing antibody (2 μg/ml) for 0 or 8 hr as indicated, were analyzed by EMSA to determine NF-κB activity using a probe containing an NF-κB DNA binding site. Oct-1 DNA binding activities were determined as loading controls.

(B) EMSA was performed to determine the specificity of inducible RelA/p50 NF-κB DNA binding activity. Competition and supershift assays were performed using 20 μg of nuclear protein from mPDAC-2 cells as indicated.

(C) Western blot was performed to determine the expression of p62 in mPDAC cells (CTL), mPDAC cells (*p62-shRNA*) expressing *p62shRNA*, and mPDAC cells (*SB-shRNA*) expressing scrambled control shRNA with anti-p62 antibody. Relative protein loading was determined by the use of anti-β-actin antibody.

Our results show that TSC1 and FOXO3a pathways are involved in Kras-induced PDAC (Figures S4G and S4H), consistent with the studies showing that IKK2/β phosphorylates TSC1 at Ser^{487} and Ser^{511} and FOXO3a for promoting tumorigenesis (Hu et al., 2004; Lee et al., 2007). Interestingly, expression of both IL-1α and IL-1β was inhibited in our *Pdx1-Cre;Kras$^{LSL-G12D}$; IKK2/β$^{F/F}$* mouse model (Figures 4E–4F), pointing out different regulatory mechanisms of IL-1β in pancreas as NF-κB activity inhibits the release of IL-1β from macrophage (Greten et al., 2007).

In summary, we report here constitutive NF-κB activation is required for PDAC development and proposed the mechanism for NF-κB activation by Kras^{G12D} through AP-1-induced IL-1α overexpression. Since IL-1α overexpression correlates with poor survival in PDAC patients, and since it is found in other diseases, such as chronic inflammation autoimmune disorders (Gabay et al., 2010), pharmacologic targeting IL-1α overexpression may represent a potential therapy for PDAC.

EXPERIMENTAL PROCEDURES

Generation of Mouse Strain

The genetically engineered mouse strains used in our study were kindly and generously provided by the following laboratories: floxed *IKK2/β* (*IKK2/β$^{F/F}$*) mice by Michael Karin's laboratory (Li et al., 2003); floxed Ink4a/Arf (*Ink4a/Arf$^{F/F}$*) mice by Ronald Depinho's laboratory (Aguirre et al., 2003); *Kras$^{LSL-G12D}$* mice by Tyler Jacks' laboratory (Johnson et al., 2001); and *Pdx1-Cre* transgenic mice by Douglas Melton's laboratory (Gu et al., 2002). These strains were interbred to generate the experimental cohorts, which include the following genotypes: *Pdx1-Cre;Kras$^{LSL-G12D}$*, *Pdx1-Cre;IKK2/β$^{F/F}$*, *Pdx1-Cre;Kras$^{LSL-G12D}$; IKK2/β$^{F/F}$*, *Pdx1-Cre;Kras$^{LSL-G12D}$;Ink4a/Arf$^{F/F}$* and *Pdx1-Cre;Kras$^{LSL-G12D}$;Ink4a/Arf$^{F/F}$; IKK2/β$^{F/F}$*. These mutant mouse strains were genotyped by PCR as previously described by the laboratories that generated them. All animal experiments were conducted under the protocol that was approved for this study by the Institutional Animal Care and Use Committee (IACUC) at the University of Texas MD Anderson Cancer Center.

Patient Pancreatic Ductal Adenocarcinoma and Adjacent Normal Tissues

Patient pancreatic cancer tissue microarray (TMA) was constructed and paraffin sections were obtained using the paraffin blocks from primary pancreatic ductal adenocarcinoma and paired adjacent normal tissues of 131 pancreatic cancer patients, which were collected within 1 hr after surgery under the protocol approved by the Institutional Review Board at M.D. Anderson Cancer Center, and written informed consent was obtained from patients in all cases at time of enrollment.

Cell Lines and Reagents

The human pancreatic cancer cell line AsPC-1 was purchased from the American Type Culture Collection. MDAPanc-28 was established by Marsha Frazier and Douglas B. Evans (M.D. Anderson Cancer Center). Immortalized/nontumorigenic HPDE and the hTERT-HPNE cells were described (Lee et al., 2005; Qian et al., 2005). Panc-28/ IκBαM, AsPc-1/IκBαM, HPNE/Kras, and HPDE/Kras cell lines were established in Chiao's laboratory (Qian et al., 2005). Anti-human IL-1α and IL-1β, anti-mouse IL-1α and IL-1β neutralizing antibodies, and IL-1α were obtained from R&D Systems.

Knockdown of *IKK2/β*, *p62*, *IL-1α*,*Traf6*, and *c-Fos*

To silence *IKK2/β*, *p62*, *and IL-1α* expression, DNA sequences encoding shRNAs and a scramble sequence were chosen to clone into the FG12 lentiviral vector. The mouse primary pancreatic cancer cell lines mPDAC-1 and mPDAC-2 and human PDAC cell lines Panc28 and AsPc-1 were infected by lentivirus containing the shRNA. The infected cells were sorted by green fluorescent protein after infection 4 days. The levels of target gene knockdown by shRNA were determined using immunoblotting.

Statistical Analysis

Mean values between groups were compared by Excel. Survival curves were plotted by the Kaplan-Meier method and compared by the log-rank test using GraphPad Prism. The correlative relationships between two quantitative measurements were investigated using Spearman rank-order correlation and the chi-square statistic. Data were analyzed by the Student t test and results were considered significant at a p value < 0.05.

ACCESSION NUMBERS

Microarray data has been deposited in the Gene Expression Omnibus (GEO) database (accession number GSE33323).

SUPPLEMENTAL INFORMATION

Supplemental Information includes five figures, three tables, and Supplemental Experimental Procedures and can be found with this article online at doi:10.1016/j.ccr.2011.12.006.

ACKNOWLEDGMENTS

We thank Dr. Michael Karin for the *IKK2/β$^{F/F}$* mice, Dr. Douglas Melton for the *Pdx1-Cre* transgenic mice, Dr. Tyler Jacks for the *Kras$^{LSL-G12D}$* mice,

(D) NF-κB activities in the nuclear extracts of mPDAC cells (*CTL*), mPDAC cells (*p62-shRNA*) expressing *p62shRNA*, and mPDAC cells (*SB-shRNA*) expressing scrambled control shRNA stimulated with IL-1α for the times indicated were determined by EMSA. Oct-1 DNA binding activities were determined as loading controls in (A) and (D).

(E) NF-κB-dependent expression of p62 was determined by western blot analysis in protein extracts from MDAPanc-28 and AsPc-1 cells expressing a Flag-tagged IκBα mutant (*Flag-IκBαM*) and their control cells expressing a puromycin resistance vector (*CTL/Puro*). Flag-IκBαM expression was verified by using anti-Flag antibody. Relative protein loading was determined by the use of anti-β-actin antibody.

(F) IL-1α-regulated p62 expression was determined by real-time PCR in MDAPanc-28, AsPc-1, mPDAC-1, and mPDAC-2 treated with anti-IL-1α neutralizing antibody (2 μg/ml) for 8 hr or IL-1α (10 ng/ml) for 1 hr as indicated.

(G) IKK2/β-induced p62 expression was determined by western blot analysis using MDAPanc-28, AsPc-1, mPDAC-1, and mPDAC-2 cells expressing *IKK2/β-shRNA* (*IKK2-shRNA*) and their control cells expressing a puromycin resistance vector (*CTL/Puro*) and scrambled shRNA (*CTL-shRNA*). IKK2/β expression was verified by using anti-IKK2/β antibody. Relative protein loading was determined by the use of anti-β-actin antibody.

(H) IL-1α-regulated p62 expression was determined by western blot analysis in protein extracts of MDAPanc-28, AsPc-1, mPDAC-1, and mPDAC-2 cells treated with anti-IL-1α neutralizing antibody (2 μg/ml) for 8 hr or IL-1α (10 ng/ml) for 1 hr as indicated. Relative protein loading was determined by using anti-β-actin antibody.

(I) The sequence alignment between mouse and human *p62* promoter regions was presented with AP-1 and NF-κB binding sites indicated.

(J) The activities of the AP-1 and κB binding sites in mouse *p62* promoter were determined. mPDAC cells were stimulated with IL-1α for one hour and ChIP assays were performed with anti-c-Fos and anti-p65/NF-κB antibodies and IgG as negative control by using real-time PCR.

(K) Analysis of p62 promoter activities in mPDAC-1 cells. The luciferase reporter gene activities are presented with the schematic illustration of the different luciferase reporter constructs of the p62 promoter constructs with mutated AP-1 and κB binding sites and control plasmids as indicated. Luciferase activity was measured as described in Experimental Procedures. Error bars represent ±SD from three independent experiments. See also Figure S4.

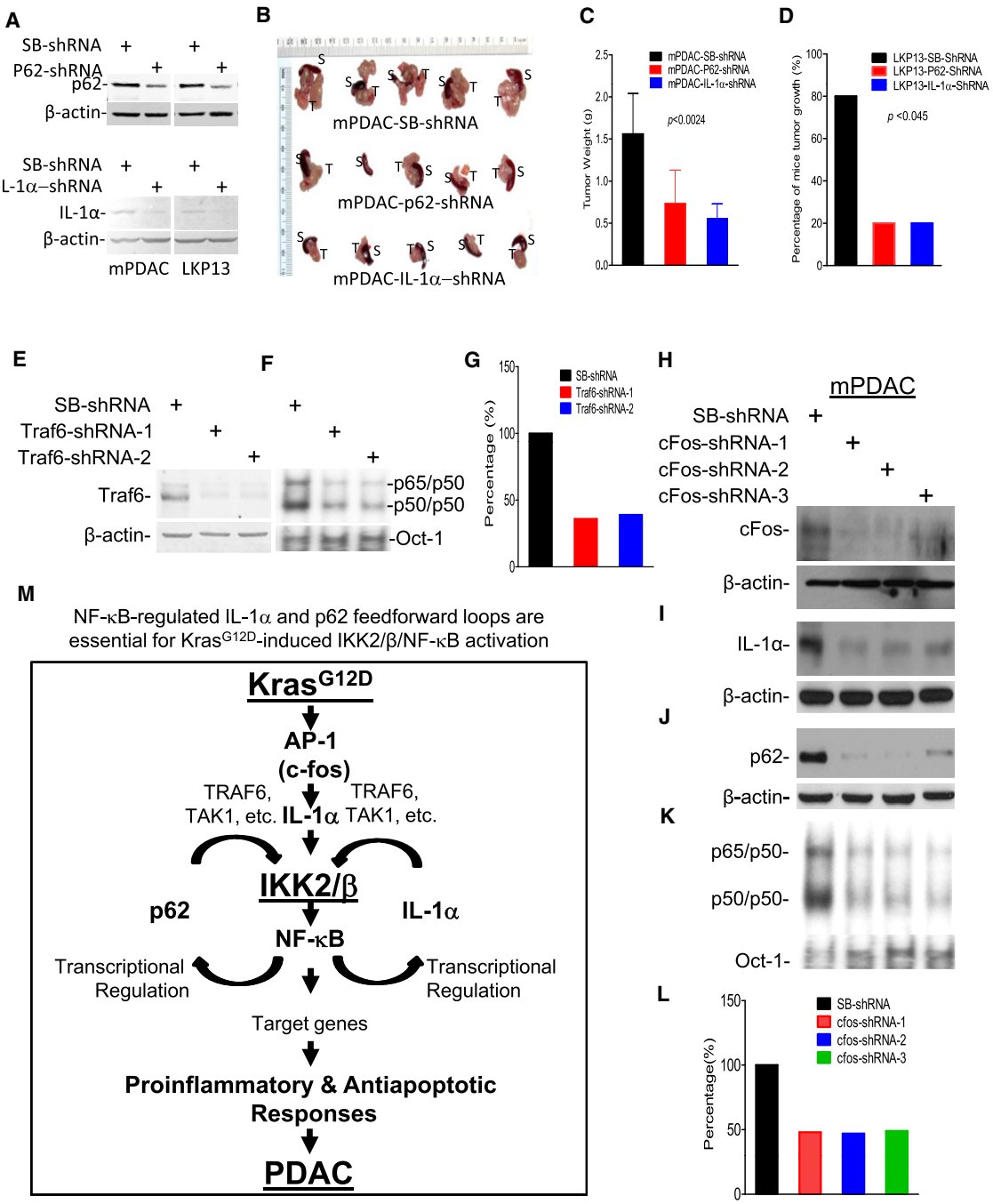

Figure 8. AP-1 Induced by Oncogenic *Kras^{G12D}* Initiates Feedforward Loops of IL-1α and p62 to Induce and Sustain Constitutive NF-κB Activation and the Working Model

(A) Knocked down expression of IL-1α and p62 in mPDAC and LKP-13 cells. The expression levels of p62 and IL-1α in mPDAC *and* LKP-13 cells expressing scrambled shRNA (*SBshRNA*), *p62shRNA,* and IL-1α*shRNA* was determined using anti-p62 or anti- IL-1α antibody in western blot with β-actin as relative protein loading controls.

(B) The resected orthotopic tumors attached to spleen in fifteen C57B6 mice injected with mPDAC-*SBshRNA*, mPDAC-*p62shRNA*, and mPDAC-*IL-1αshRNA* cells (n = 5 per group) were shown at week 5. S: spleen; T: tumor.

(C) Tumor weight in C57B6 mice orthotopically injected with mPDAC-*SBshRNA*, mPDAC-*p62shRNA*, and mPDAC-*IL-1αshRNA* cells. Columns: mean of all individual tumors in each group. Error bars: ±SD of the pancreatic tumor from five mice in each of the three groups as indicated.

(D) Percentage of C57B6 mice that developed subcutaneous tumors after injection of *LKP-13-SB-shRNA, LKP-13-p62shRNA*, and *LKP-13-IL-1αshRNA* cells. Columns: percentage of the mice that grew tumor in each group (n = 5). The statistical significance was determined by Fisher's exact test.

(E) Expression of TRAF6 in mPDAC cells expressing scrambled Traf6 shRNA (*SB-shRNA*) and two Traf6-shRNA (*Traf6-shRNA-1 and 2*) was determined by anti-TRAF6 antibody with β-actin as loading control.

Dr. Ronald DePinho for the *Ink4a/Arf* $^{F/F}$ mice, and Dr. Kenneth Hess in the Department of Biostatistics, M.D. Anderson Cancer Center, for statistical analysis, Dr. Chang-gong Liu in Sequencing & Non-coding RNA Program and Dr. Wei Zhang at Genomic Core, M.D. Anderson Cancer Center, for microarray analysis. We also thank Yu (June) Cao for technical assistance and Kathryn Hale for editorial assistance. The work was supported in part by grants from the National Cancer Institute (CA109405 and CA142674 to P.J.C.), a Cancer Center Core Supporting grant (CA16672), and Sister Institution Fund of China Medical University and Hospital and MD Anderson Cancer Center to M. C. H.

Received: June 20, 2011
Revised: November 2, 2011
Accepted: December 13, 2011
Published: January 17, 2012

REFERENCES

Aguirre, A.J., Bardeesy, N., Sinha, M., Lopez, L., Tuveson, D.A., Horner, J., Redston, M.S., and DePinho, R.A. (2003). Activated Kras and Ink4a/Arf deficiency cooperate to produce metastatic pancreatic ductal adenocarcinoma. Genes Dev. *17*, 3112–3126.

Barbie, D.A., Tamayo, P., Boehm, J.S., Kim, S.Y., Moody, S.E., Dunn, I.F., Schinzel, A.C., Sandy, P., Meylan, E., Scholl, C., et al. (2009). Systematic RNA interference reveals that oncogenic KRAS-driven cancers require TBK1. Nature *462*, 108–112.

Bardeesy, N., Aguirre, A.J., Chu, G.C., Cheng, K.H., Lopez, L.V., Hezel, A.F., Feng, B., Brennan, C., Weissleder, R., Mahmood, U., et al. (2006). Both p16(Ink4a) and the p19(Arf)-p53 pathway constrain progression of pancreatic adenocarcinoma in the mouse. Proc. Natl. Acad. Sci. USA *103*, 5947–5952.

Bassères, D.S., Ebbs, A., Levantini, E., and Baldwin, A.S. (2010). Requirement of the NF-kappaB subunit p65/RelA for K-Ras-induced lung tumorigenesis. Cancer Res. *70*, 3537–3546.

Brentnall, T.A., Bronner, M.P., Byrd, D.R., Haggitt, R.C., and Kimmey, M.B. (1999). Early diagnosis and treatment of pancreatic dysplasia in patients with a family history of pancreatic cancer. Ann. Intern. Med. *131*, 247–255.

Chien, Y., Kim, S., Bumeister, R., Loo, Y.M., Kwon, S.W., Johnson, C.L., Balakireva, M.G., Romeo, Y., Kopelovich, L., Gale, M., Jr., et al. (2006). RalB GTPase-mediated activation of the IkappaB family kinase TBK1 couples innate immune signaling to tumor cell survival. Cell *127*, 157–170.

Dajee, M., Lazarov, M., Zhang, J.Y., Cai, T., Green, C.L., Russell, A.J., Marinkovich, M.P., Tao, S., Lin, Q., Kubo, Y., and Khavari, P.A. (2003). NF-kappaB blockade and oncogenic Ras trigger invasive human epidermal neoplasia. Nature *421*, 639–643.

Duran, A., Linares, J.F., Galvez, A.S., Wikenheiser, K., Flores, J.M., Diaz-Meco, M.T., and Moscat, J. (2008). The signaling adaptor p62 is an important NF-kappaB mediator in tumorigenesis. Cancer Cell *13*, 343–354.

Fujioka, S., Sclabas, G.M., Schmidt, C., Niu, J., Frederick, W.A., Dong, Q.G., Abbruzzese, J.L., Evans, D.B., Baker, C., and Chiao, P.J. (2003). Inhibition of constitutive NF-kappa B activity by I kappa B alpha M suppresses tumorigenesis. Oncogene *22*, 1365–1370.

Gabay, C., Lamacchia, C., and Palmer, G. (2010). IL-1 pathways in inflammation and human diseases. Nat. Rev. Rheumatol. *6*, 232–241.

Greten, F.R., Arkan, M.C., Bollrath, J., Hsu, L.C., Goode, J., Miething, C., Göktuna, S.I., Neuenhahn, M., Fierer, J., Paxian, S., et al. (2007). NF-kappaB is a negative regulator of IL-1beta secretion as revealed by genetic and pharmacological inhibition of IKKbeta. Cell *130*, 918–931.

Gu, G., Dubauskaite, J., and Melton, D.A. (2002). Direct evidence for the pancreatic lineage: NGN3+ cells are islet progenitors and are distinct from duct progenitors. Development *129*, 2447–2457.

He, G., Yu, G.Y., Temkin, V., Ogata, H., Kuntzen, C., Sakurai, T., Sieghart, W., Peck-Radosavljevic, M., Leffert, H.L., and Karin, M. (2010). Hepatocyte IKKbeta/NF-kappaB inhibits tumor promotion and progression by preventing oxidative stress-driven STAT3 activation. Cancer Cell *17*, 286–297.

Hingorani, S.R., Petricoin, E.F., Maitra, A., Rajapakse, V., King, C., Jacobetz, M.A., Ross, S., Conrads, T.P., Veenstra, T.D., Hitt, B.A., et al. (2003). Preinvasive and invasive ductal pancreatic cancer and its early detection in the mouse. Cancer Cell *4*, 437–450.

Hruban, R.H., Goggins, M., Parsons, J., and Kern, S.E. (2000). Progression model for pancreatic cancer. Clin. Cancer Res. *6*, 2969–2972.

Hu, M.C., Lee, D.F., Xia, W., Golfman, L.S., Ou-Yang, F., Yang, J.Y., Zou, Y., Bao, S., Hanada, N., Saso, H., et al. (2004). IkappaB kinase promotes tumorigenesis through inhibition of forkhead FOXO3a. Cell *117*, 225–237.

Johnson, L., Mercer, K., Greenbaum, D., Bronson, R.T., Crowley, D., Tuveson, D.A., and Jacks, T. (2001). Somatic activation of the K-ras oncogene causes early onset lung cancer in mice. Nature *410*, 1111–1116.

Karin, M. (2008). The IkappaB kinase - a bridge between inflammation and cancer. Cell Res. *18*, 334–342.

Kim, M.P., Evans, D.B., Wang, H., Abbruzzese, J.L., Fleming, J.B., and Gallick, G.E. (2009). Generation of orthotopic and heterotopic human pancreatic cancer xenografts in immunodeficient mice. Nat. Protoc. *4*, 1670–1680.

Lee, D.F., Kuo, H.P., Chen, C.T., Hsu, J.M., Chou, C.K., Wei, Y., Sun, H.L., Li, L.Y., Ping, B., Huang, W.C., et al. (2007). IKK beta suppression of TSC1 links inflammation and tumor angiogenesis via the mTOR pathway. Cell *130*, 440–455.

Lee, K.M., Yasuda, H., Hollingsworth, M.A., and Ouellette, M.M. (2005). Notch 2-positive progenitors with the intrinsic ability to give rise to pancreatic ductal cells. Lab. Invest. *85*, 1003–1012.

Li, Z.W., Omori, S.A., Labuda, T., Karin, M., and Rickert, R.C. (2003). IKK beta is required for peripheral B cell survival and proliferation. J. Immunol. *170*, 4630–4637.

Lomaga, M.A., Yeh, W.C., Sarosi, I., Duncan, G.S., Furlonger, C., Ho, A., Morony, S., Capparelli, C., Van, G., Kaufman, S., et al. (1999). TRAF6 deficiency results in osteopetrosis and defective interleukin-1, CD40, and LPS signaling. Genes Dev. *13*, 1015–1024.

Lowenfels, A.B., Maisonneuve, P., DiMagno, E.P., Elitsur, Y., Gates, L.K., Jr., Perrault, J., and Whitcomb, D.C.; International Hereditary Pancreatitis Study

(F) NF-κB activities in the nuclear extracts of mPDAC cells expressing scrambled Traf6 shRNA (*SB-shRNA*) and two *Traf6-shRNAs* were determined by EMSA. Oct-1 DNA binding activities were determined as loading controls.
(G) Quantitation of NFκB activities in EMSA by Image Analysis Software (ImageQuant TL 7.0).
(H) c-Fos expression in mPDAC expressing a scrambled control shRNA (*SB-shRNA*) and three different cFos-shRNAs (*cfos-shRNA-1, 2, 3*) was determined with anti-cFos antibody in western blot analysis.
(I) The levels of IL-1α in mPDAC cytoplasmic extracts expressing a scrambled control shRNA (*SB-shRNA*) and three different cFos-shRNAs (c-*fos*-shRNA-1, 2, 3) were analyzed by anti-IL-1α western blot with β-actin as loading control.
(J) p62 expression in mPDAC cells expressing a scrambled control shRNA(*SB-shRNA*), and three different cFos-shRNAs (*cfos-shRNA-1, 2, 3*) were analyzed by anti-p62 western blot with β-actin as loading control.
(K) NF-κB activity from mPDAC expressing a scrambled control shRNA(*SB-shRNA*) and three different cFos-shRNAs (*cfos-shRNA-1, 2, 3*) were analyzed by EMSA. Oct-1 DNA binding activities were determined as loading controls
(L) Quantitation of NFκB activities in EMSA by Image Analysis Software (ImageQuant TL 7.0).
(M) A proposed working model illustrates the potential mechanism through which *Kras^{G12D}* oncogenic signaling induces feedforward loops of IL-1α and p62 to sustain constitutive IKK2/β/NF-κB activation in PDAC development. See also Figure S5.

Group. (1997). Hereditary pancreatitis and the risk of pancreatic cancer. J. Natl. Cancer Inst. *89*, 442–446.

Maeda, S., Kamata, H., Luo, J.L., Leffert, H., and Karin, M. (2005). IKKbeta couples hepatocyte death to cytokine-driven compensatory proliferation that promotes chemical hepatocarcinogenesis. Cell *121*, 977–990.

Meylan, E., Dooley, A.L., Feldser, D.M., Shen, L., Turk, E., Ouyang, C., and Jacks, T. (2009). Requirement for NF-kappaB signalling in a mouse model of lung adenocarcinoma. Nature *462*, 104–107.

Mori, N., and Prager, D. (1996). Transactivation of the interleukin-1alpha promoter by human T-cell leukemia virus type I and type II Tax proteins. Blood *87*, 3410–3417.

Naito, A., Azuma, S., Tanaka, S., Miyazaki, T., Takaki, S., Takatsu, K., Nakao, K., Nakamura, K., Katsuki, M., Yamamoto, T., and Inoue, J. (1999). Severe osteopetrosis, defective interleukin-1 signalling and lymph node organogenesis in TRAF6-deficient mice. Genes Cells *4*, 353–362.

Osborn, L., Kunkel, S., and Nabel, G.J. (1989). Tumor necrosis factor alpha and interleukin 1 stimulate the human immunodeficiency virus enhancer by activation of the nuclear factor kappa B. Proc. Natl. Acad. Sci. USA *86*, 2336–2340.

Peng, B., Ling, J., Lee, A.J., Wang, Z., Chang, Z., Jin, W., Kang, Y., Zhang, R., Shim, D., Wang, H., et al. (2010). Defective feedback regulation of NF-kappaB underlies Sjogren's syndrome in mice with mutated kappaB enhancers of the IkappaBalpha promoter. Proc. Natl. Acad. Sci. USA *107*, 15193–15198.

Pomerantz, J.L., and Baltimore, D. (1999). NF-kappaB activation by a signaling complex containing TRAF2, TANK and TBK1, a novel IKK-related kinase. EMBO J. *18*, 6694–6704.

Qian, J., Niu, J., Li, M., Chiao, P.J., and Tsao, M.S. (2005). In vitro modeling of human pancreatic duct epithelial cell transformation defines gene expression changes induced by K-ras oncogenic activation in pancreatic carcinogenesis. Cancer Res. *65*, 5045–5053.

Sanz, L., Diaz-Meco, M.T., Nakano, H., and Moscat, J. (2000). The atypical PKC-interacting protein p62 channels NF-kappaB activation by the IL-1-TRAF6 pathway. EMBO J. *19*, 1576–1586.

Skaug, B., Jiang, X., and Chen, Z.J. (2009). The role of ubiquitin in NF-kappaB regulatory pathways. Annu. Rev. Biochem. *78*, 769–796.

Staudt, L.M. (2010). Oncogenic activation of NF-kappaB. Cold Spring Harb. Perspect. Biol. *2*, a000109.

Tuveson, D.A., Shaw, A.T., Willis, N.A., Silver, D.P., Jackson, E.L., Chang, S., Mercer, K.L., Grochow, R., Hock, H., Crowley, D., et al. (2004). Endogenous oncogenic K-ras(G12D) stimulates proliferation and widespread neoplastic and developmental defects. Cancer Cell *5*, 375–387.

Wang, C., Deng, L., Hong, M., Akkaraju, G.R., Inoue, J., and Chen, Z.J. (2001). TAK1 is a ubiquitin-dependent kinase of MKK and IKK. Nature *412*, 346–351.

Wang, W., Abbruzzese, J.L., Evans, D.B., Larry, L., Cleary, K.R., and Chiao, P.J. (1999). The nuclear factor-kappa B RelA transcription factor is constitutively activated in human pancreatic adenocarcinoma cells. Clin. Cancer Res. *5*, 119–127.

Wislez, M., Spencer, M.L., Izzo, J.G., Juroske, D.M., Balhara, K., Cody, D.D., Price, R.E., Hittelman, W.N., Wistuba, I.I., and Kurie, J.M. (2005). Inhibition of mammalian target of rapamycin reverses alveolar epithelial neoplasia induced by oncogenic K-ras. Cancer Res. *65*, 3226–3235.

Wooten, M.W., Geetha, T., Seibenhener, M.L., Babu, J.R., Diaz-Meco, M.T., and Moscat, J. (2005). The p62 scaffold regulates nerve growth factor-induced NF-kappaB activation by influencing TRAF6 polyubiquitination. J. Biol. Chem. *280*, 35625–35629.

Yang, J., Splittgerber, R., Yull, F.E., Kantrow, S., Ayers, G.D., Karin, M., and Richmond, A. (2010). Conditional ablation of Ikkb inhibits melanoma tumor development in mice. J. Clin. Invest. *120*, 2563–2574.

Zabel, U., Henkel, T., Silva, M.S., and Baeuerle, P.A. (1993). Nuclear uptake control of NF-kappa B by MAD-3, an I kappa B protein present in the nucleus. EMBO J. *12*, 201–211.